



# The neutral upper atmosphere

## thermosphere and exosphere

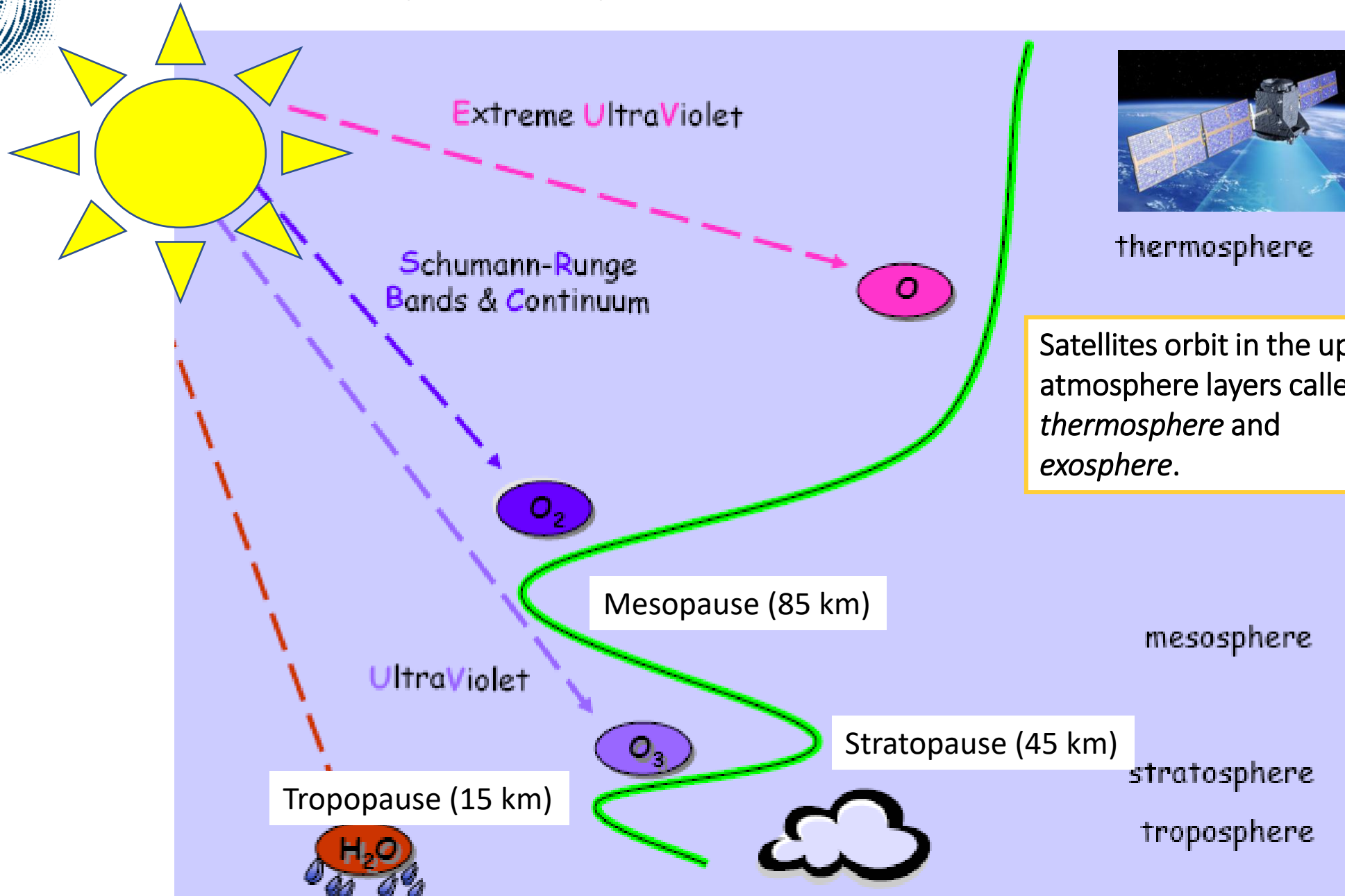


Sean Bruinsma  
CNES, Space Geodesy Office, Toulouse, France

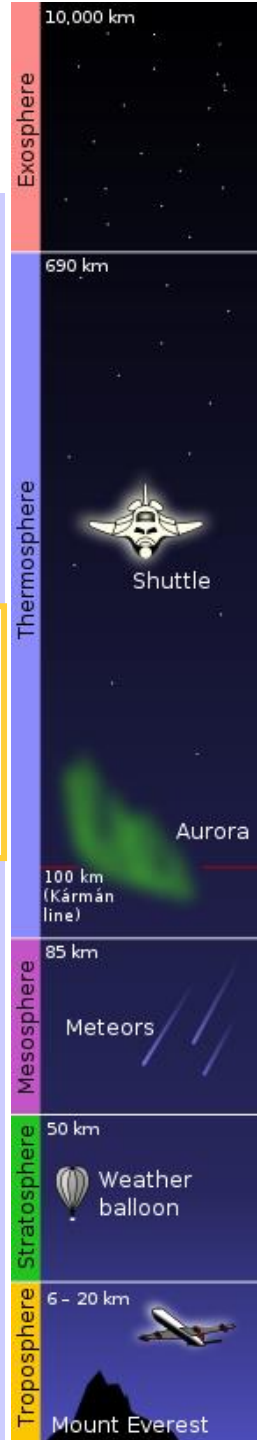
PITHIA Training School  
KU Leuven, 6 February 2024



# Earth's atmosphere layers

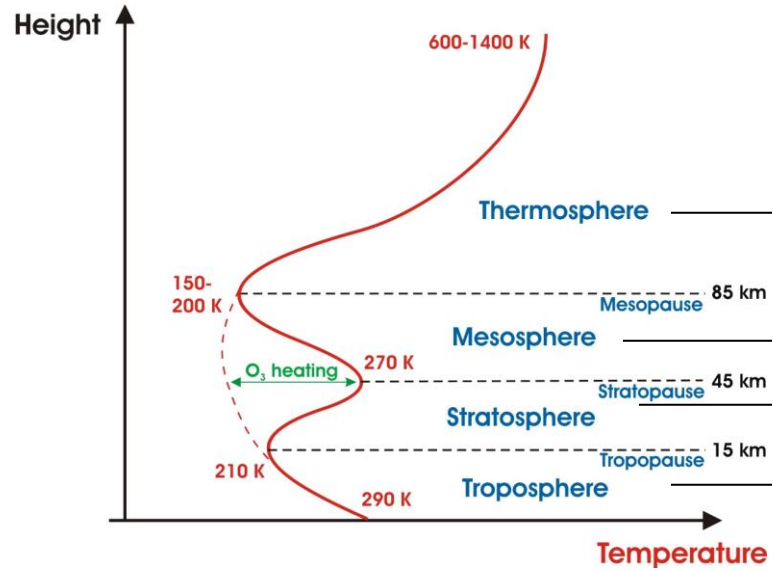


Satellites orbit in the upper atmosphere layers called *thermosphere* and *exosphere*.





# Global Mean Energy Sources and Sinks



**Troposphere:**

- **Energy sources:**
  - Planetary surface absorption (IR, visible), convection & conduction to atmosphere
  - Atmospheric absorption of terrestrial and solar IR
  - Latent heat release by H<sub>2</sub>O
- **Energy sinks:**
  - IR radiation
  - Evaporation of H<sub>2</sub>O

**Thermosphere:**

- **Energy sources:**
  - Absorption of EUV (20-100 nm; photoionizing O, O<sub>2</sub>, N<sub>2</sub>) and UV (120-200 nm; photodissociating O<sub>2</sub>), leading to chemical reactions and particle collisions, liberating energy
  - Joule heating by auroral electrical currents
  - Particle precipitation from the magnetosphere
  - Dissipation of upward propagating waves (tides, planetary waves, gravity waves)
- **Energy sinks:**
  - Thermal conduction into the mesosphere, where energy is radiated by CO<sub>2</sub>, O<sub>3</sub> and H<sub>2</sub>O
  - IR cooling by CO<sub>2</sub>, NO, O

**Mesosphere:**

- **Energy sources:**
  - Some UV absorption by O<sub>3</sub> (lower heights)
  - Heat transport down from thermosphere (minor, upper heights only)
  - Chemical heating
- **Energy sinks:**
  - IR radiation by CO<sub>2</sub>, H<sub>2</sub>O, OH

**Stratosphere:**

- **Energy sources:**
  - Strong absorption of UV by ozone (causing stratopause temperature peak)
- **Energy sinks:**
  - IR radiation by O<sub>3</sub>, CO<sub>2</sub>, H<sub>2</sub>O



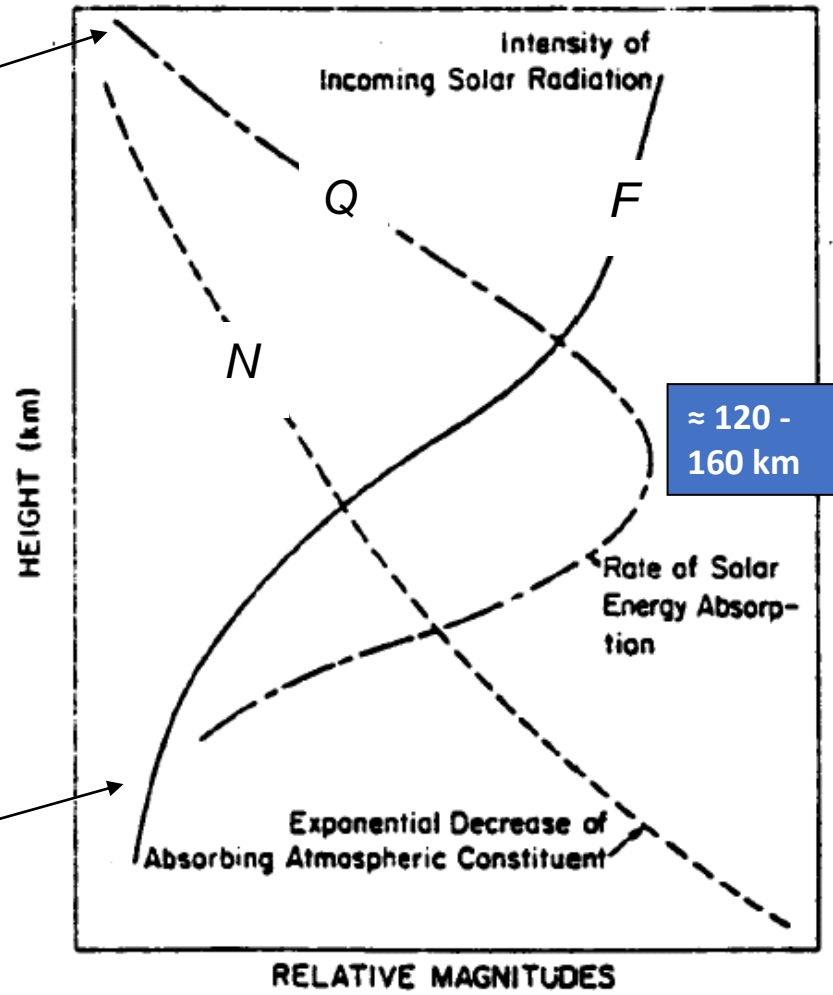
# Solar Radiation Absorption in the Thermosphere

Absorbing gas is thin here; therefore little absorption.

Three factors determine the rate of solar radiation absorption,  $Q$ :

- No. of photons (solar flux,  $F$ )
- No. of absorbing molecules,  $N$
- Efficiency of absorption (cross-section)

Few photons left here; therefore little absorption.





# Hydrostatic equilibrium

$n$  = # molecules per unit volume

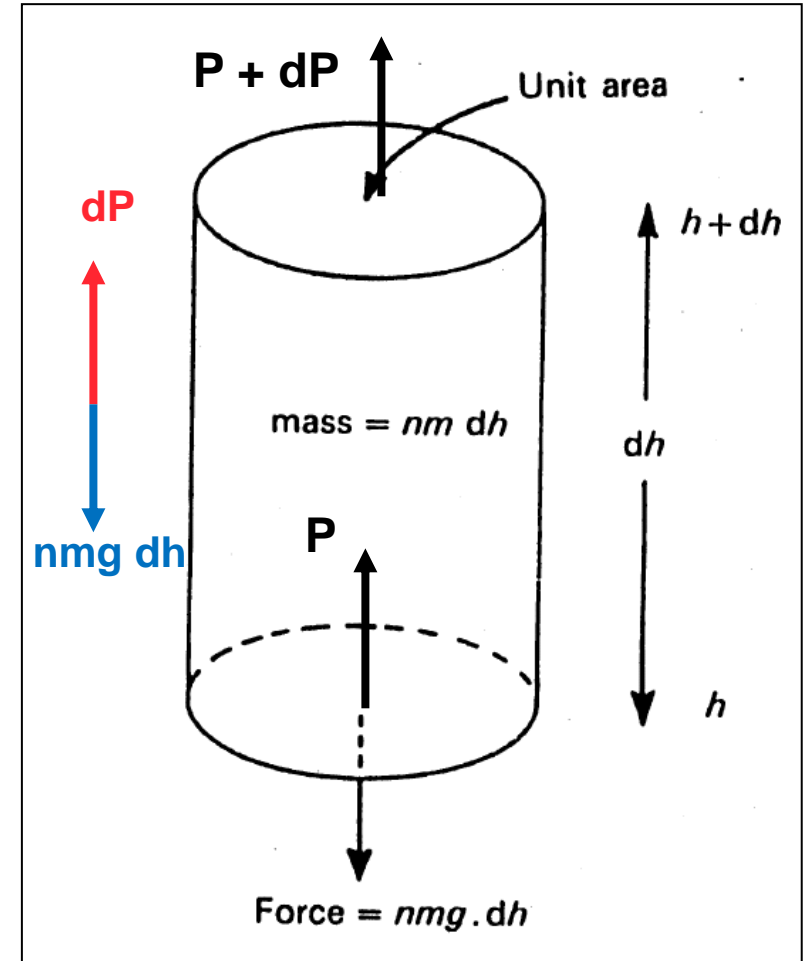
$m$  = mass of each particle

$nm dh$  = total mass contained in a cylinder of air (of unit cross-sectional area)

The force due to gravity  $g$  on the cylindrical mass is:  $nmg dh$

The difference in pressure between the upper and lower faces of the cylinder balances the above force in an equilibrium situation:

$$(P + dP) - P = -nmg dh$$





# Hydrostatic equilibrium

Since  $m$  varies from constituent to constituent (i.e., H, He, O, O<sub>2</sub>, N<sub>2</sub>, ...), the equations apply to individual constituents  $i$ :

$$P = P_{i0} e^{-h/H_i}$$

$$n = n_{i0} e^{-h/H_i}$$

$$\rho = \rho_{i0} e^{-h/H_i}$$

*Derivation given at the end of the presentation in A(ppendix)1*

where  $P_i$  is the partial pressure and  $H_i = \frac{kT}{m_i g}$  where  $H$  is called the scale height (general way to describe how a value fades away, it is the distance for density to drop by  $1/e = 0.37$ )

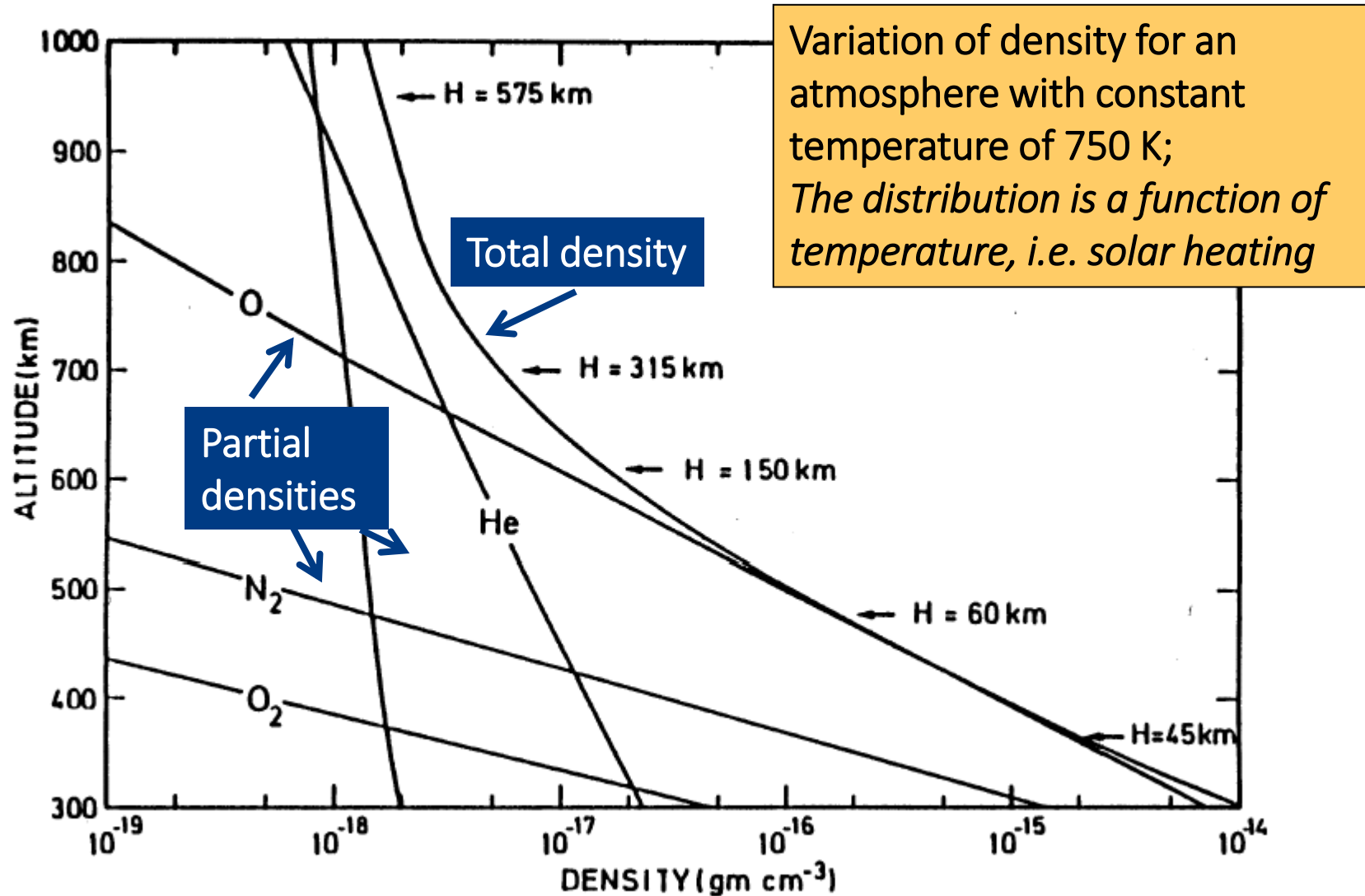
Thus, each individual constituent has the tendency to distribute vertically according to its own individual scale height (see following figure).

The process which makes this possible is molecular diffusion.



# Hydrostatic equilibrium

The total density and composition as a function of altitude





# Hydrostatic equilibrium

The efficiency of molecular diffusion increases according to the mean free path of atmospheric particles, and hence inversely with atmospheric density.

At sufficiently low altitudes in the atmosphere, molecular diffusion is not able to compete with the various mixing processes in the atmosphere (turbulent diffusion, wave and general dynamical transport, etc.).

The atmosphere, in fact, remains well-mixed below about 100 km. This regime is called the homosphere and is characterized by a constant mean molecular weight as a function of height.

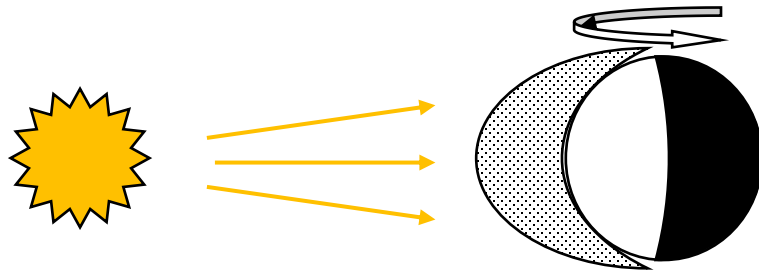
- It is not until about 100 km (the exact height is species dependent, due to the dependence of molecular diffusion velocity on mean molecular weight) that molecular diffusion begins to take over, and each species separates according to its individual scale height.
- This separation occurs at the homopause, or turbopause. Above the homopause is the heterosphere; homosphere below.



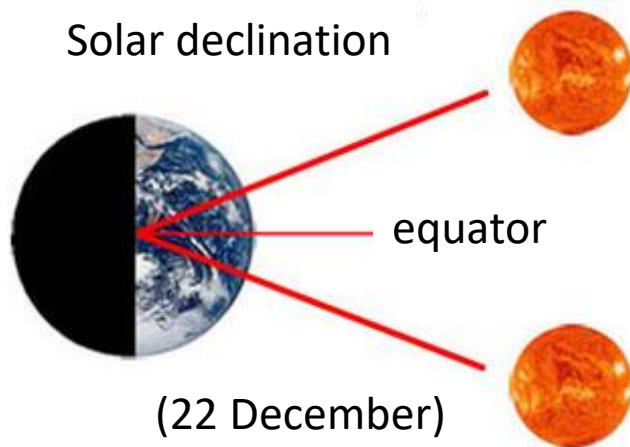
# Upper atmosphere heating

## Solar radiation – EUV emissions

Earth rotation: ('day-night' effect):



Received energy at a location is variable:



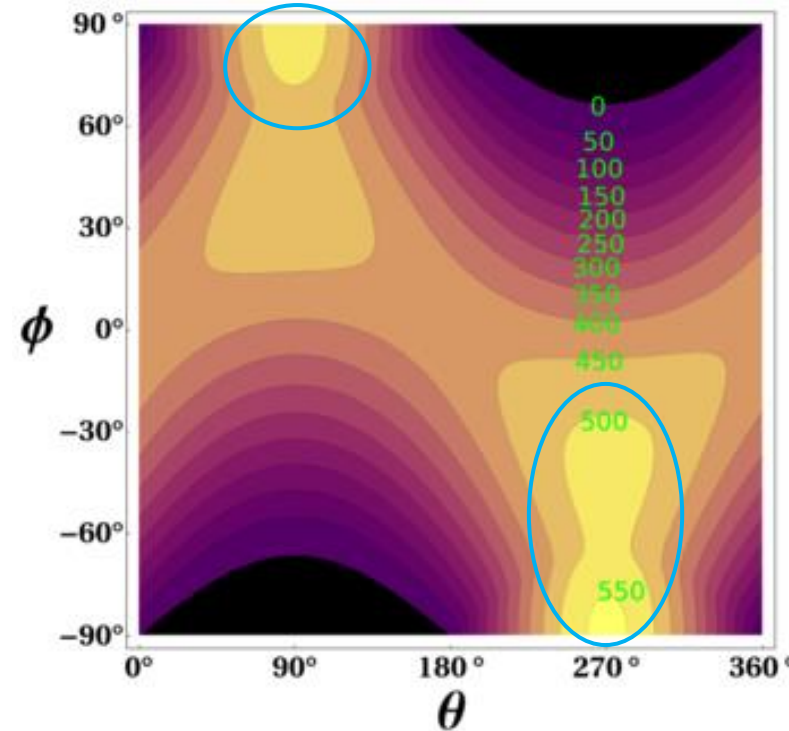
Correction due to eccentricity:  $\pm 3\%$

$$E = E_s \times (\bar{R} / r)^2 \times \cos \chi$$

Solar constant

Solar zenith angle

## Seasonal and latitudinal effects



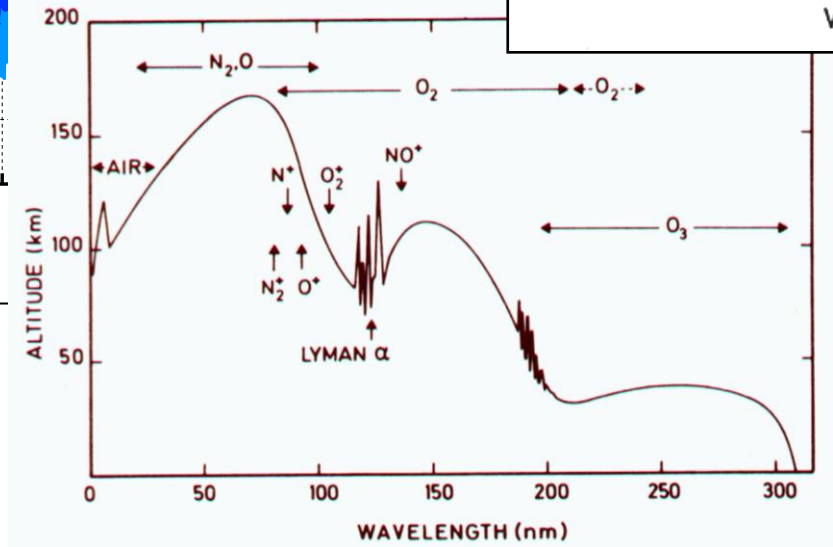
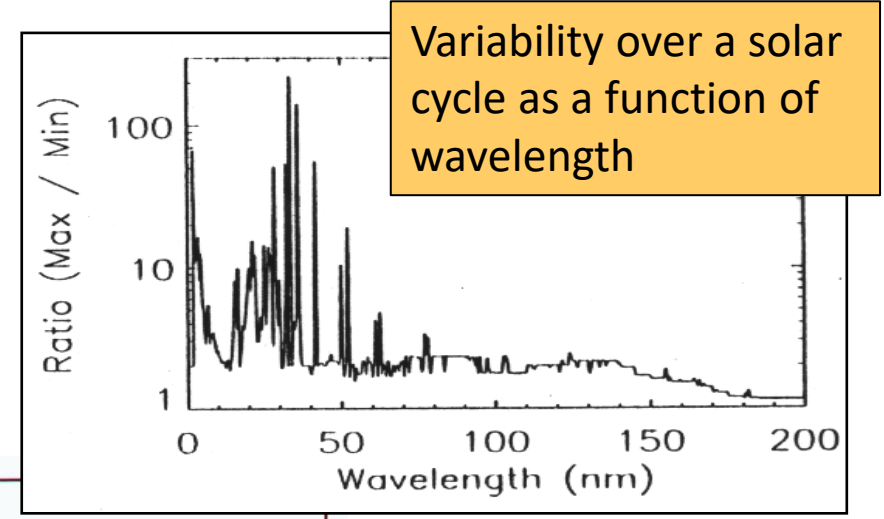
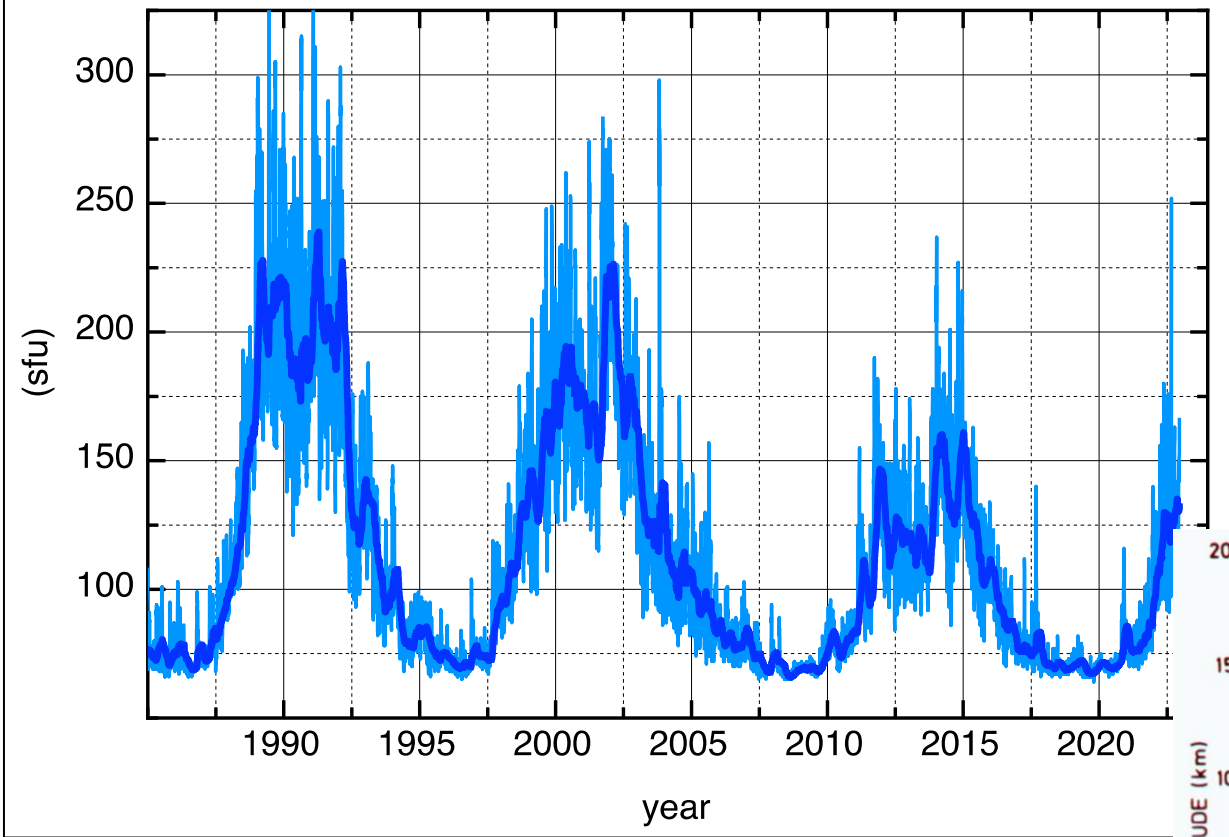
Energy deposition is unequal:  
*Perihelion is early January*



# Upper atmosphere heating

Variability in solar UV/EUV emissions: the approximately 11 year solar cycle

81-day mean and daily F10.7 solar radio flux



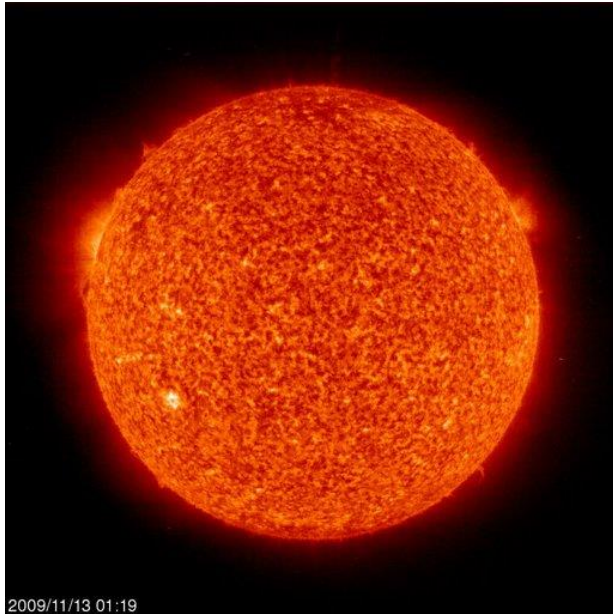
Altitude of maximum solar radiation absorption



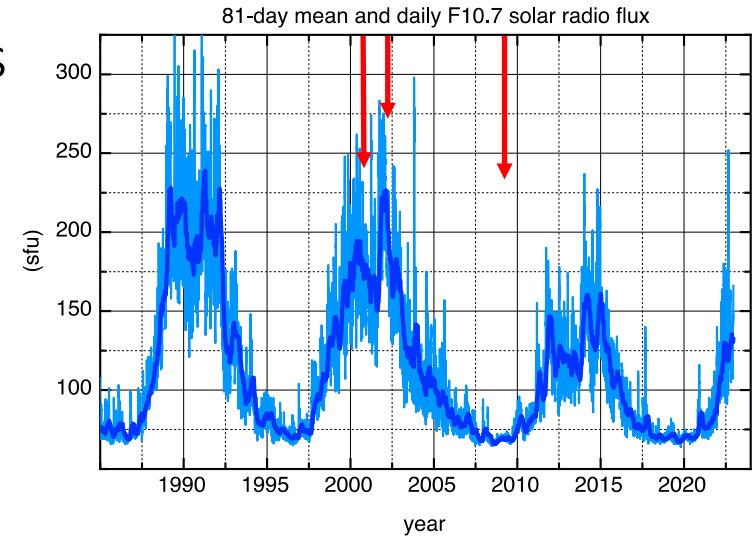
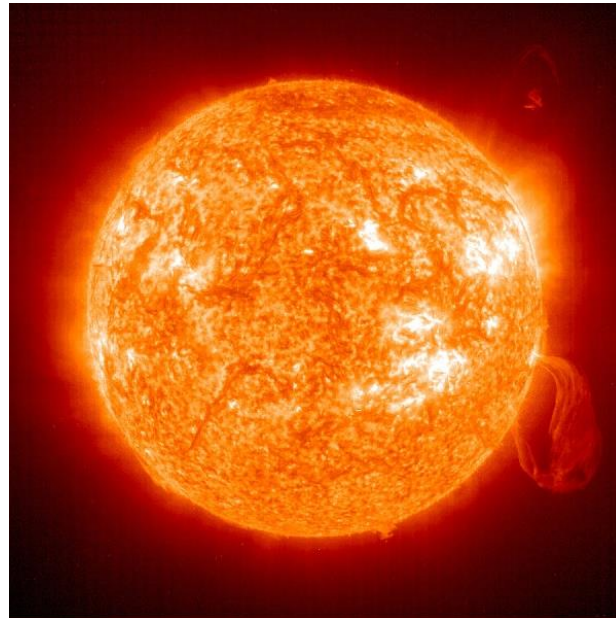
# Upper atmosphere heating

Variability in EUV (30 nm) over a solar cycle: examples

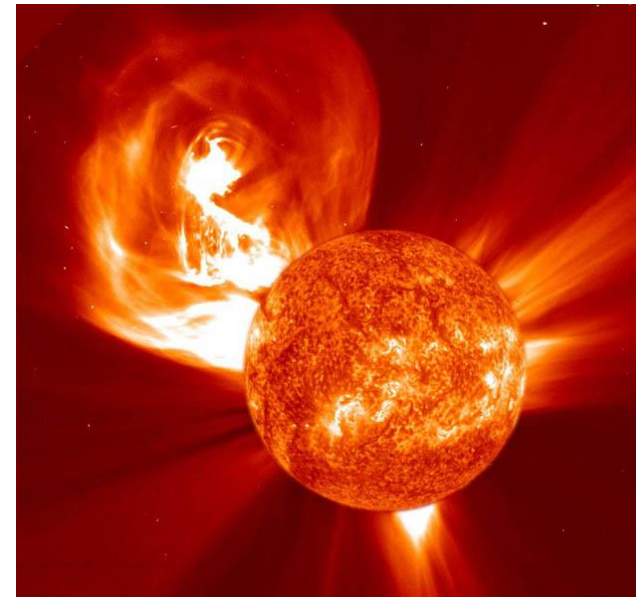
2009 (weak activity: cycle minimum)



2001 (high activity: cycle maximum)



2002 (high activity+Coronal Mass (CME))





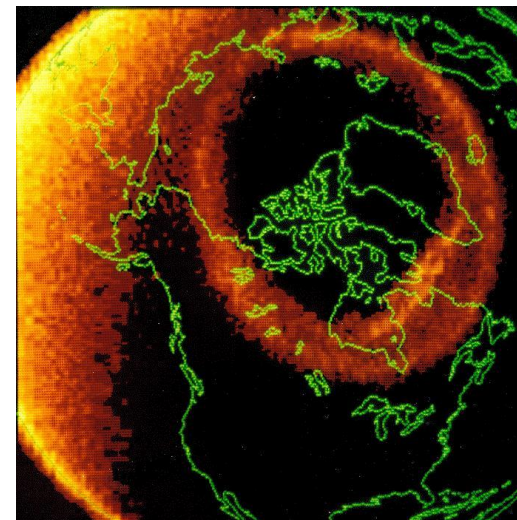
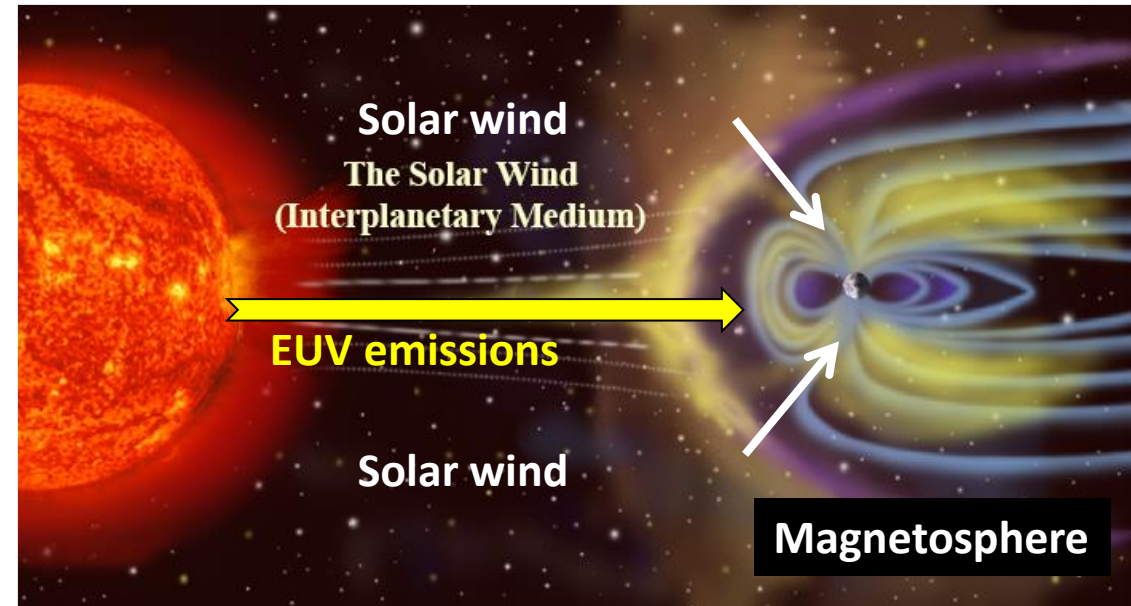
# Upper atmosphere heating

Solar wind *particles* – Magnetosphere coupling, Joule heating

Coupling between interplanetary medium and the magnetosphere depends on:

- Orientation of the interplanetary magnetic field ( $B_z$  in particular)
- Density and speed of the solar wind

Upper atmosphere heating is due to:  
'Solar activity' = EUV  
'Geomagnetic activity' = Solar wind

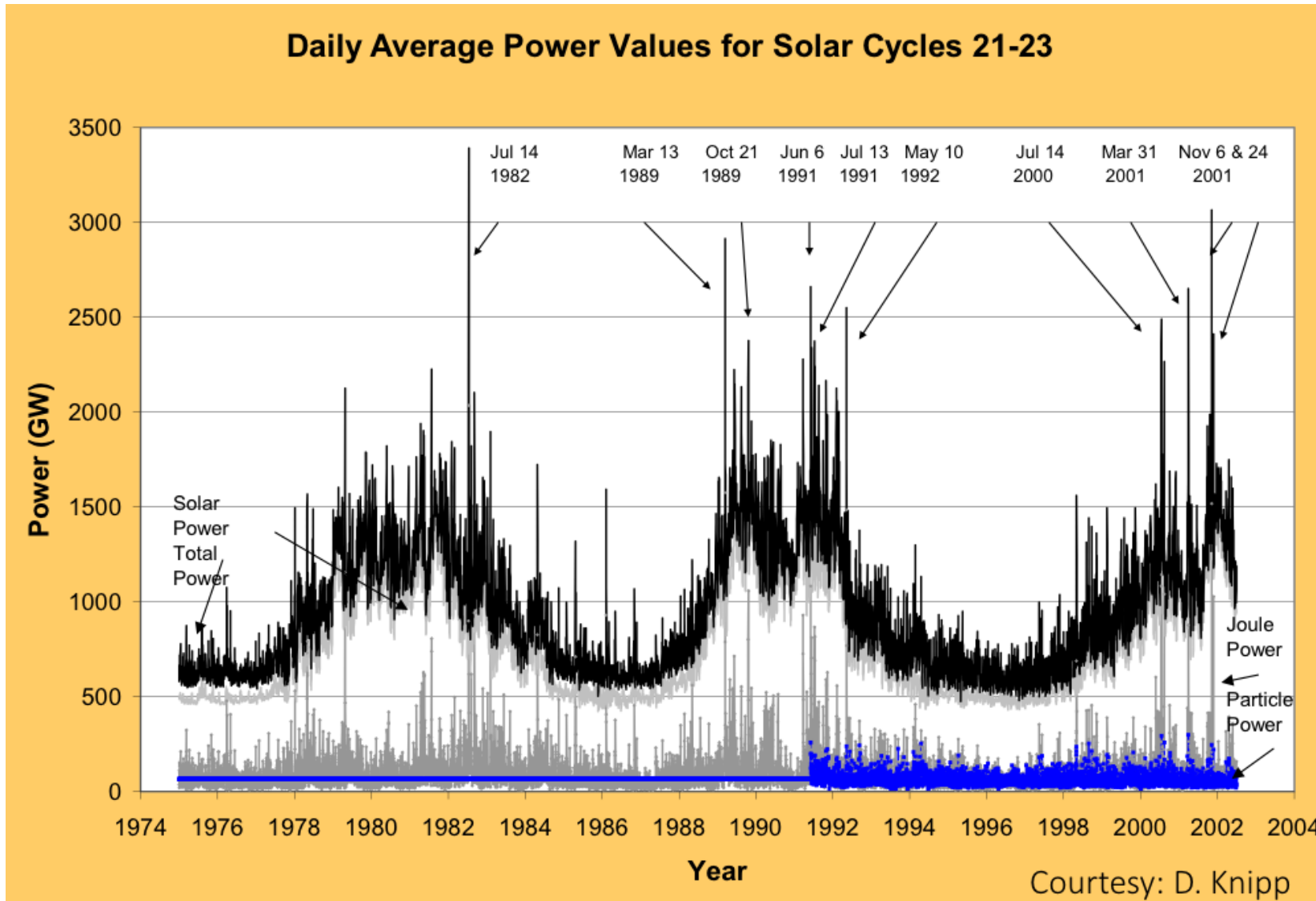


Ergo:  
Aurora visible at high latitude



# Upper atmosphere heating

Total heating = solar + geomagnetic activity





# Thermosphere models

Types: **1 - Physical**      **2 - Tabular**      **3 - Empirical**

**1 – Physical**, or first principles models: three-dimensional fluid equations are solved with a time-step of typically 1 minute

*Example: TIE-GCM (Thermosphere-Ionosphere-Electrodynamics General Circulation Model) - a global first-principles model with 2.5° latitude by longitude grid and 29 (or more) pressure level from 97km to ~600km  
(and: WAM, WACCM-X, GITM, Gaia, CTIPe)*

Inputs to TIE-GCM:

- Convection and auroral precipitation patterns from *AMIE* (Assimilative Mapping of Ionospheric Electrodynamics), Weimer, Heelis
- Solar EUV fluxes (NB: lower-resolution spectrum scaled by F10.7)
- Semidiurnal and diurnal tides from the *GSWM* (Global Scale Wave Model)

advantage:      realistic physics, variability qualitatively correct

disadvantage:      complex and costly calculation, for expert users, often no Helium

uncertainty:      ?



# Thermosphere models

Types: **1 - Physical**      **2 - Tabular**      **3 - Empirical**

## 2 - Tabular (interpolation)

*Example: MCM\* (Mowa Climatological Model) - model of the whole atmosphere by means of blending averaged data tables of the Unified Model (UM) from the Met Office for the atmosphere (0 to 120 km) and DTM2020 (120-1500 km)  
(and: GRAM, MarsGRAM\*, MCD & VCD database)*

Typical input:

- date, position
- solar flux, solar activity conditions, geomagnetic activity index (e.g. Kp)

advantage :      fast and easy calculation, simple algorithm

disadvantage :   truncated resolution, interpolations errors, limited by number of scenarios

uncertainty:      ?

\* *Combination of tabular + empirical*



# Thermosphere models

Types: **1 - Physical**      **2 - Tabular**      **3 - Empirical**

## 3 - Empirical

*Example: DTM (drag Temperature Model) - thermosphere model from 120-1500 km reproducing a limited number of known variations by fitting to observations, using a simple and fast algorithm.*

*(and: Jacchia, NRLMSIS, JB2008, Stewart Mars model, Hedin Venus model)*

input:

- date, position
- solar activity proxy or proxies (e.g. F10.7), geomagnetic activity index (e.g. Kp)

**advantage :**      fast and easy calculation, simple algorithm, robust

**disadvantage :**      low resolution, simple algorithm, highly dependent on quality of data

**uncertainty:**      8-25% ( $1\sigma$ , for Earth)

NB: despite its weaknesses, this kind of model is used in orbit computation



# Thermosphere models

Types: **1 - Physical**      **2 - Tabular**      **3 - Empirical**

1, 3 – plus data assimilation

*Example empirical model: HASDM*

*Example physical models: WAM, Gaia, Aeneas*

HASDM input:

- date, position
- solar activity proxy or proxies (F10.7), geomagnetic activity index (ap, Dst)

advantage:      idem physical/empirical models + high accuracy

disadvantage:      idem physical/empirical models + data management and quality control

uncertainty:      3-10% for HASDM; physical models ?

NB: (no) data availability is a show stopper

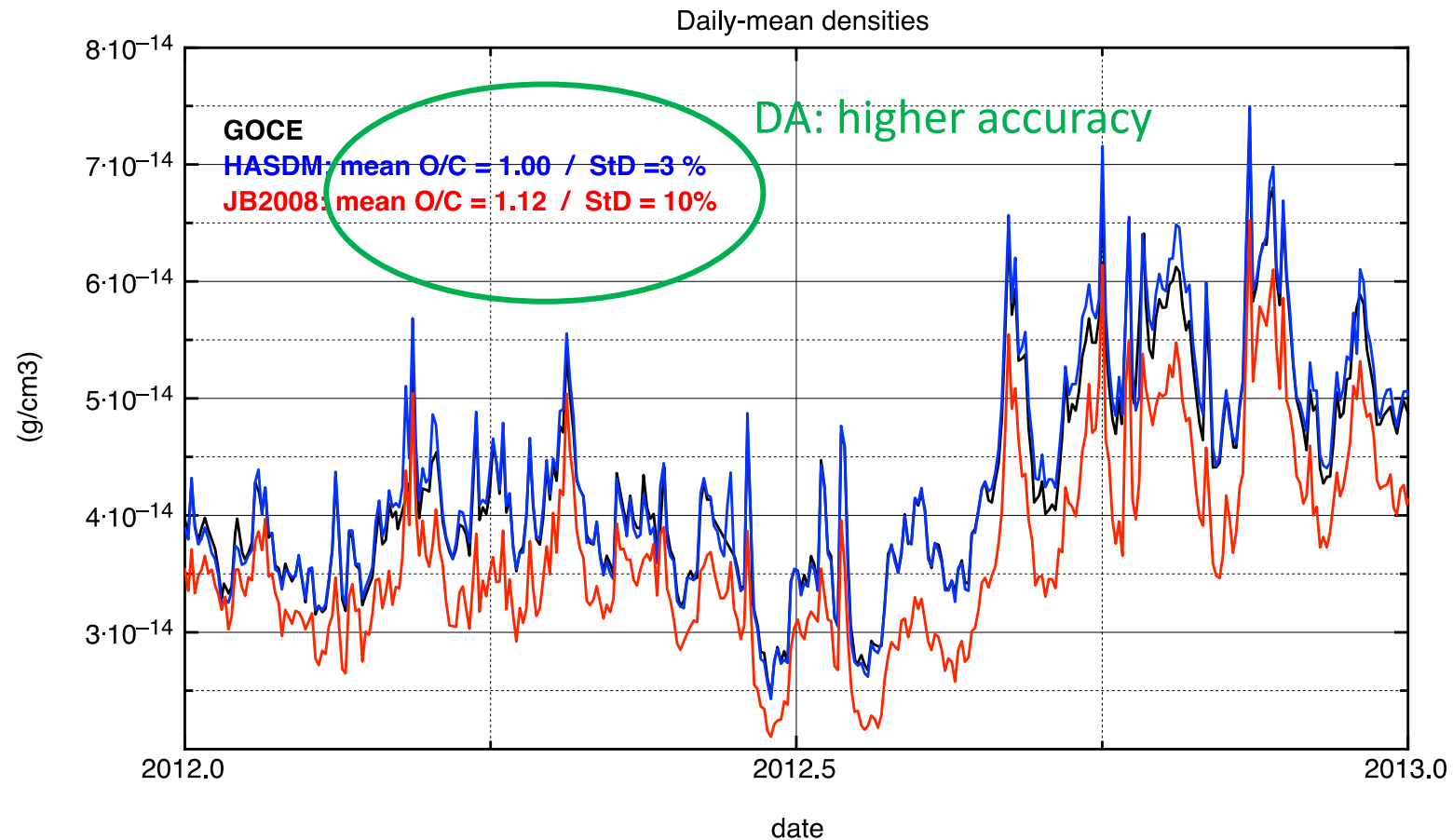


# Thermosphere models

Types: 1 - Physical      2 - Tabular      3 - Empirical

1, 3 – plus data assimilation

*Example empirical model: HASDM - comparison with GOCE densities at 255 km*

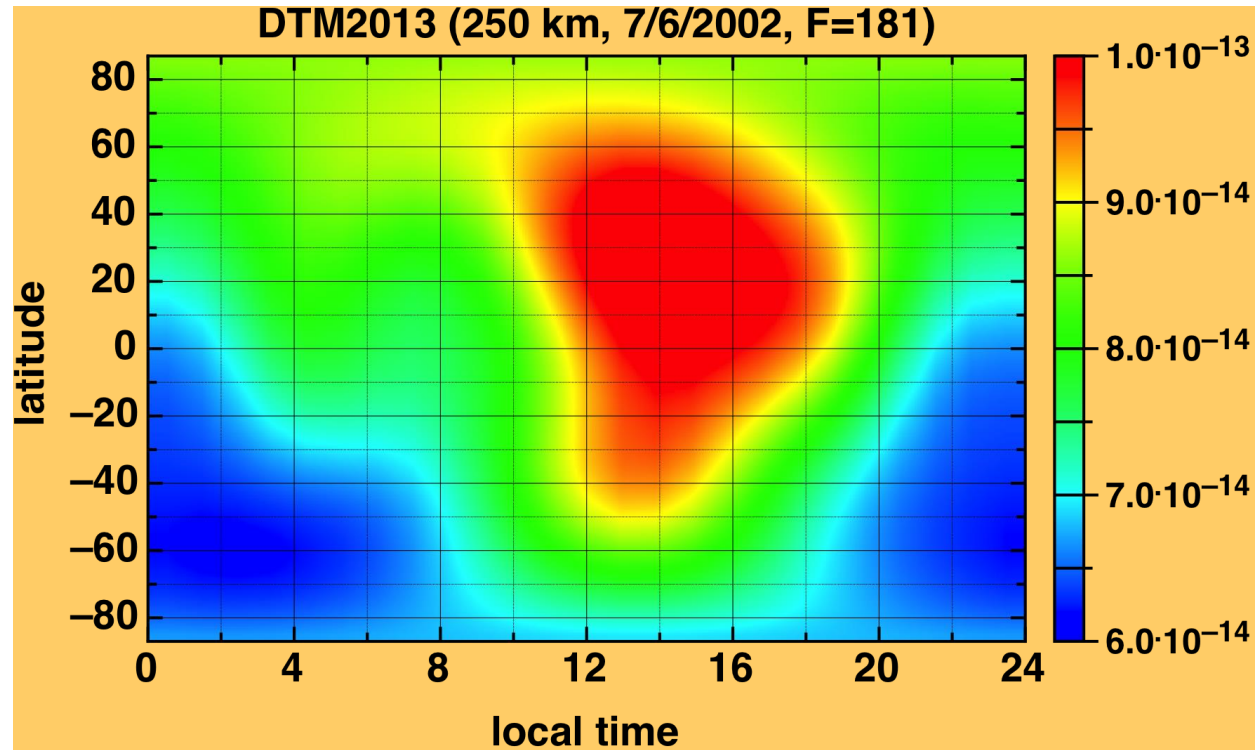
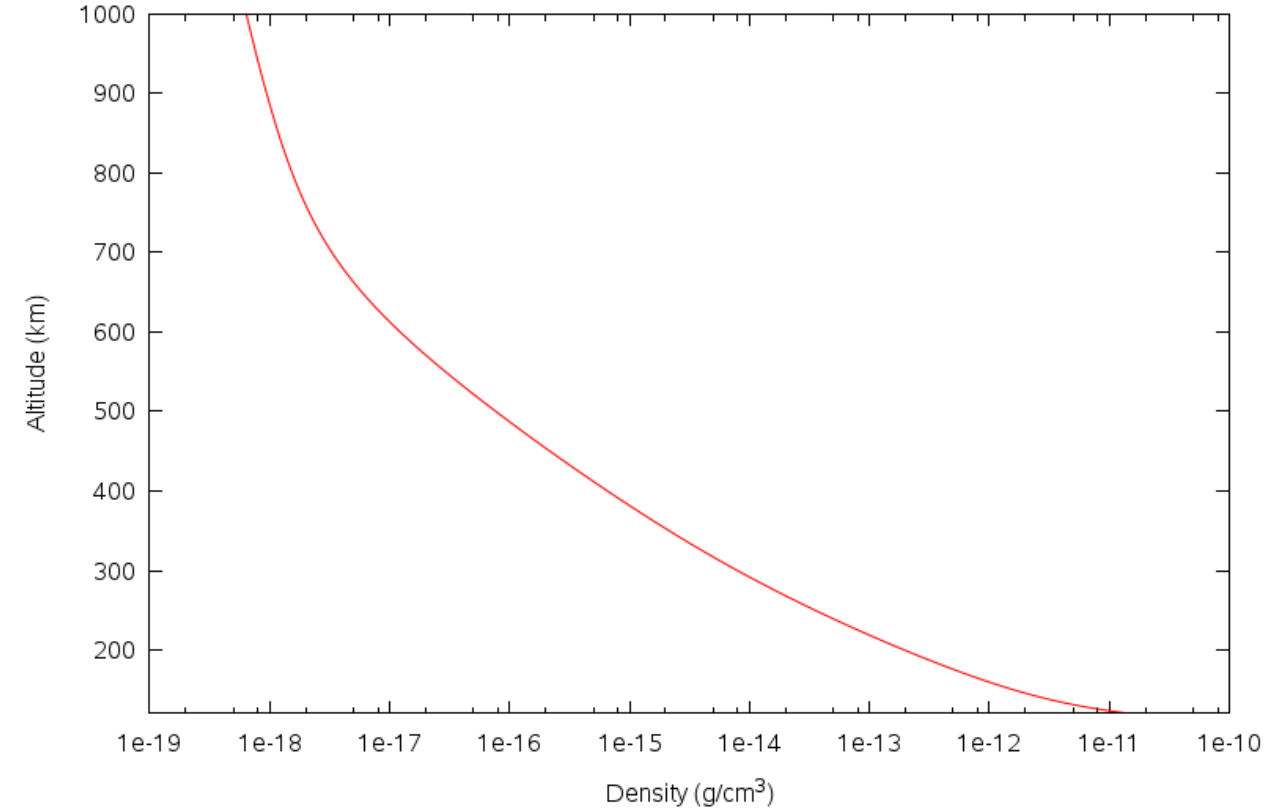




# Thermosphere density: variability

Thermosphere density is function of location:

- Altitude
- Latitude, longitude
- Local solar time

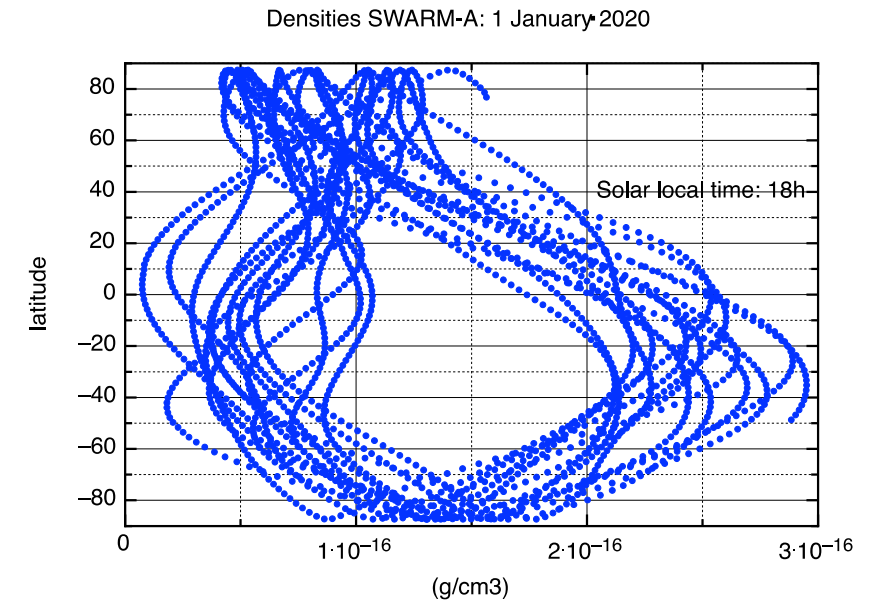
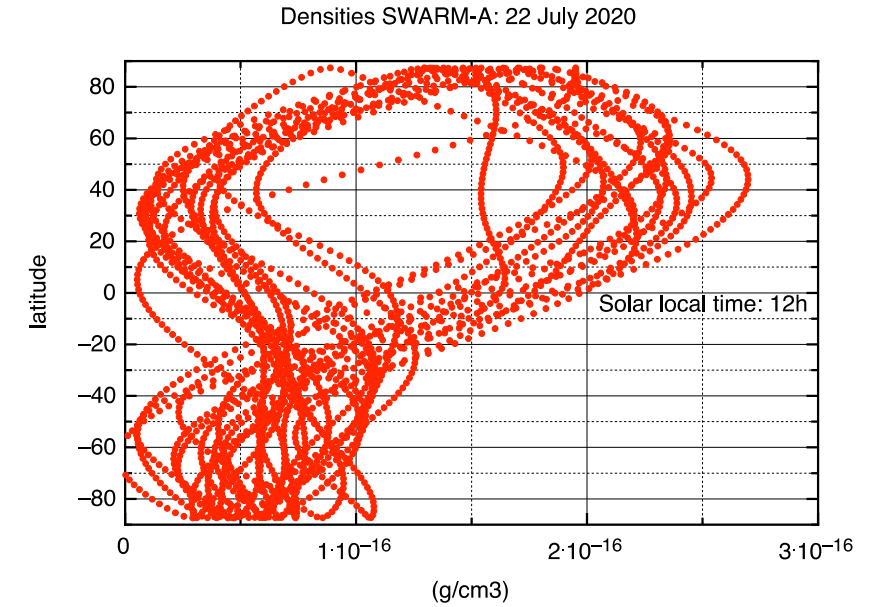
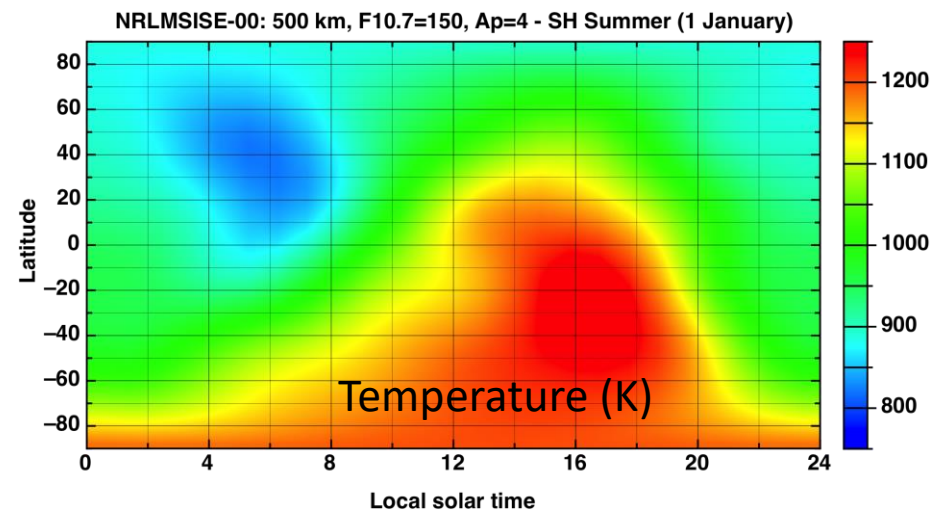
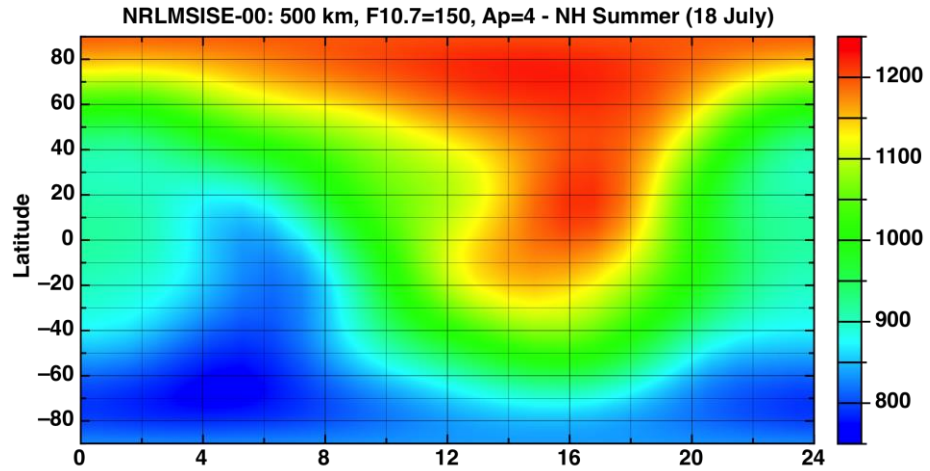
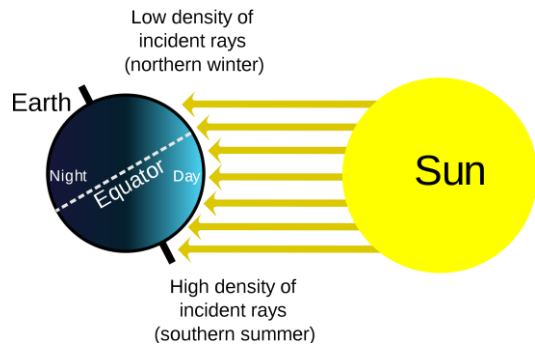




# Thermosphere density: variability

Thermosphere density is function of:

- Season





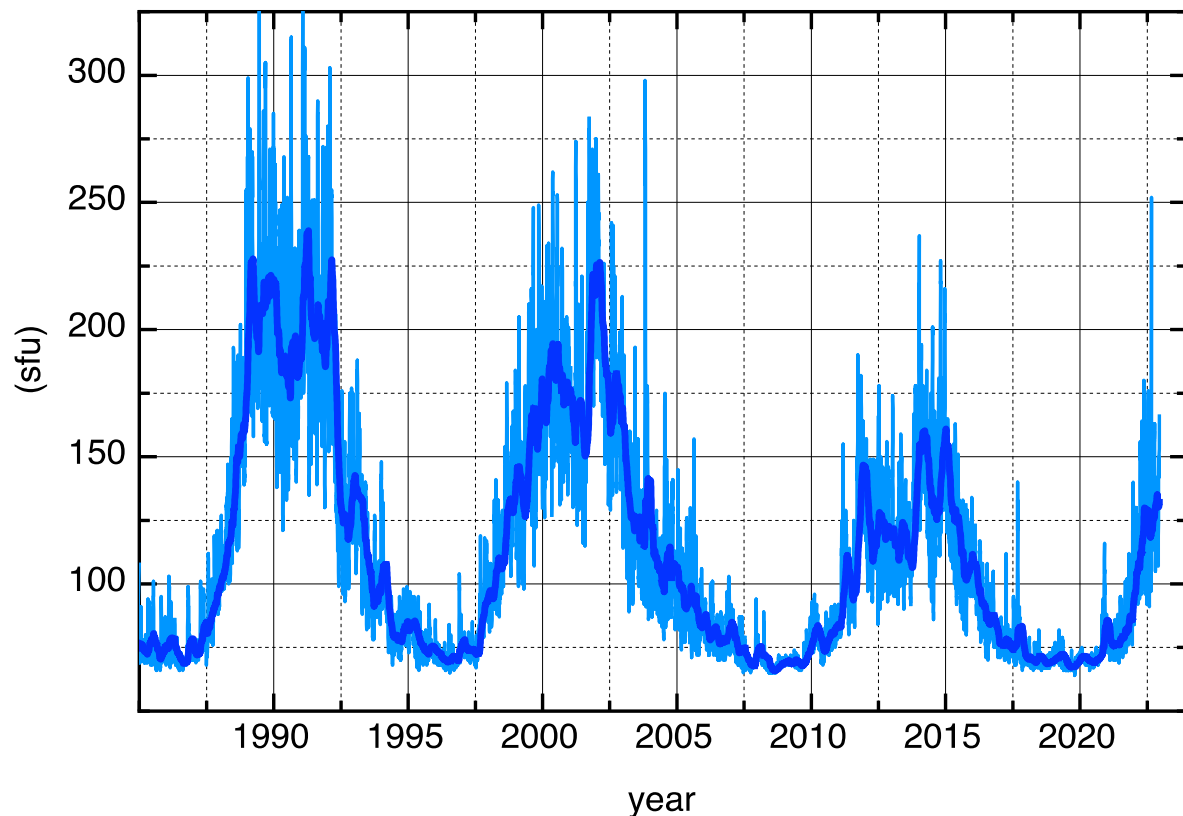
# Thermosphere density: variability

Thermosphere density is function of:

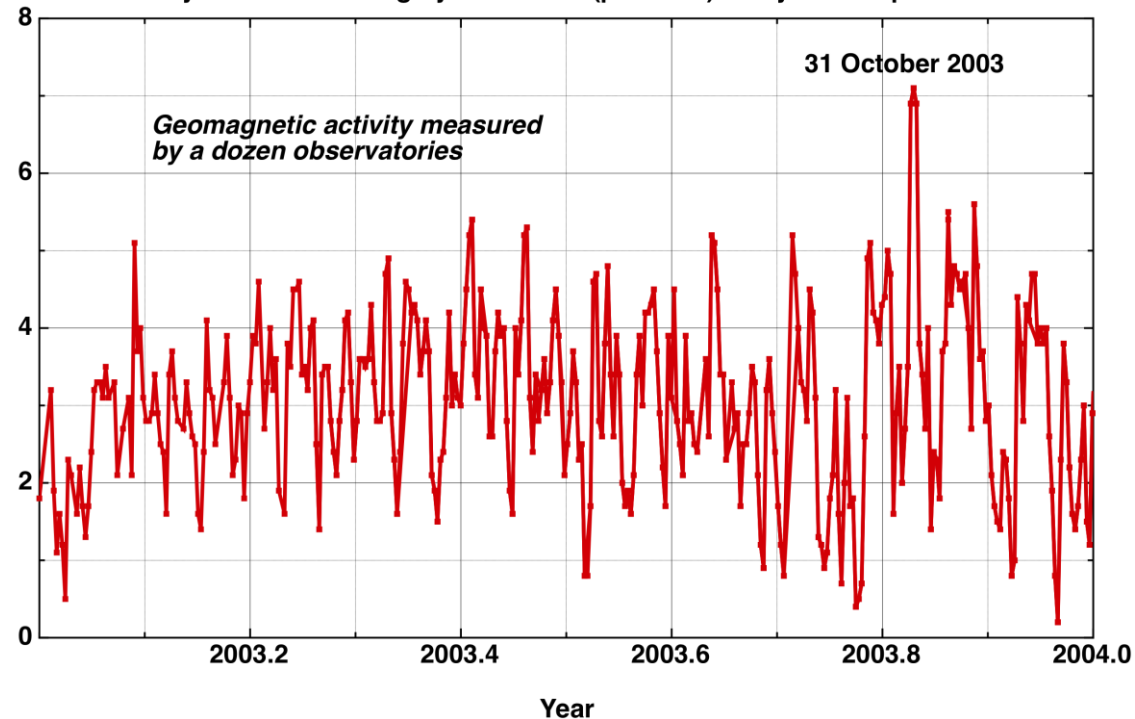
- Solar and geomagnetic activity > *proxies*

*(measurement that mimics variations of another observable)*

81-day mean and daily F10.7 solar radio flux



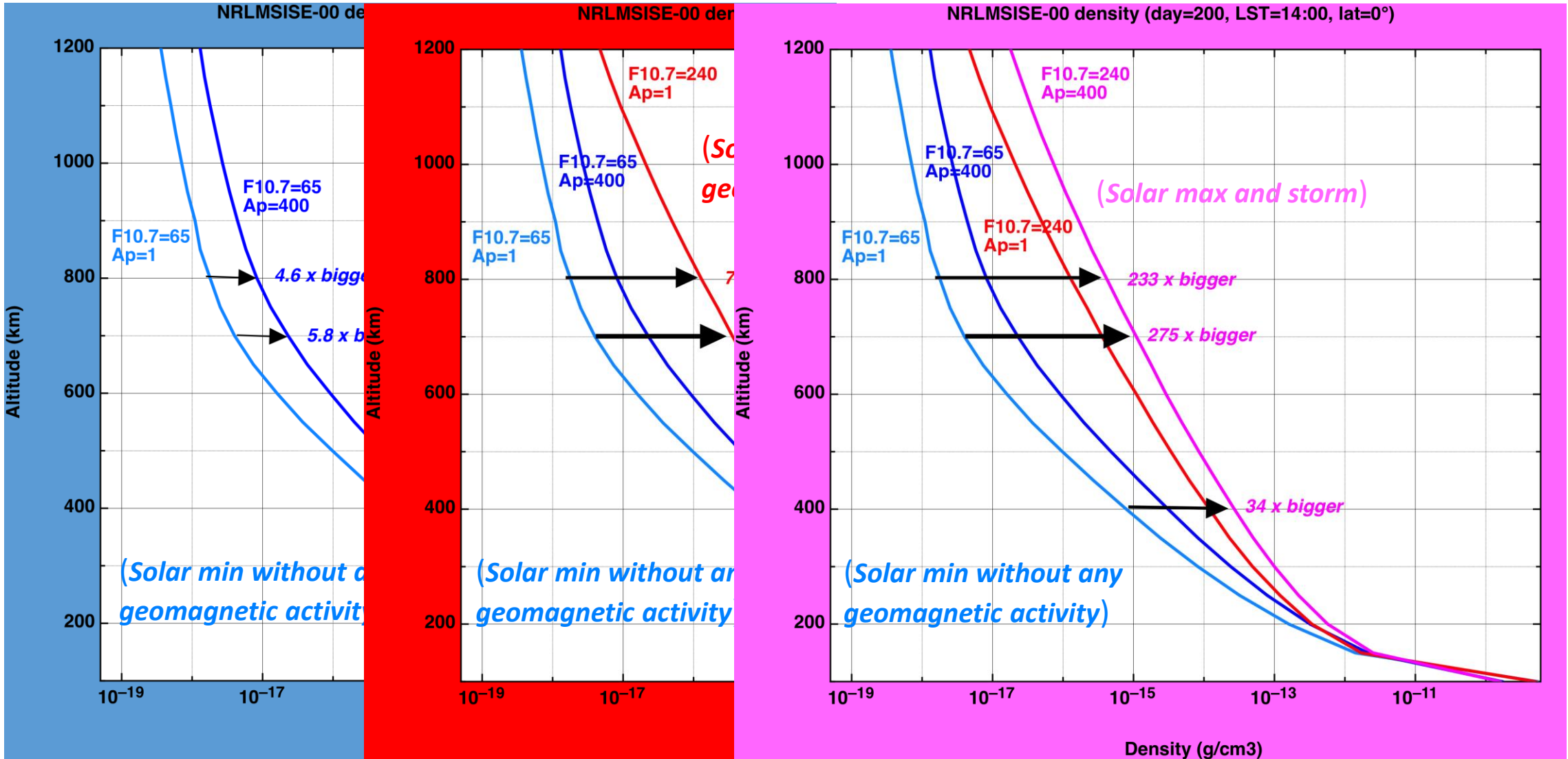
Proxy for Joule heating by solar wind (particles): daily mean Kp for 2003





# Thermosphere density: variability

Maximum versus minimum density as a function of altitude (*model*):

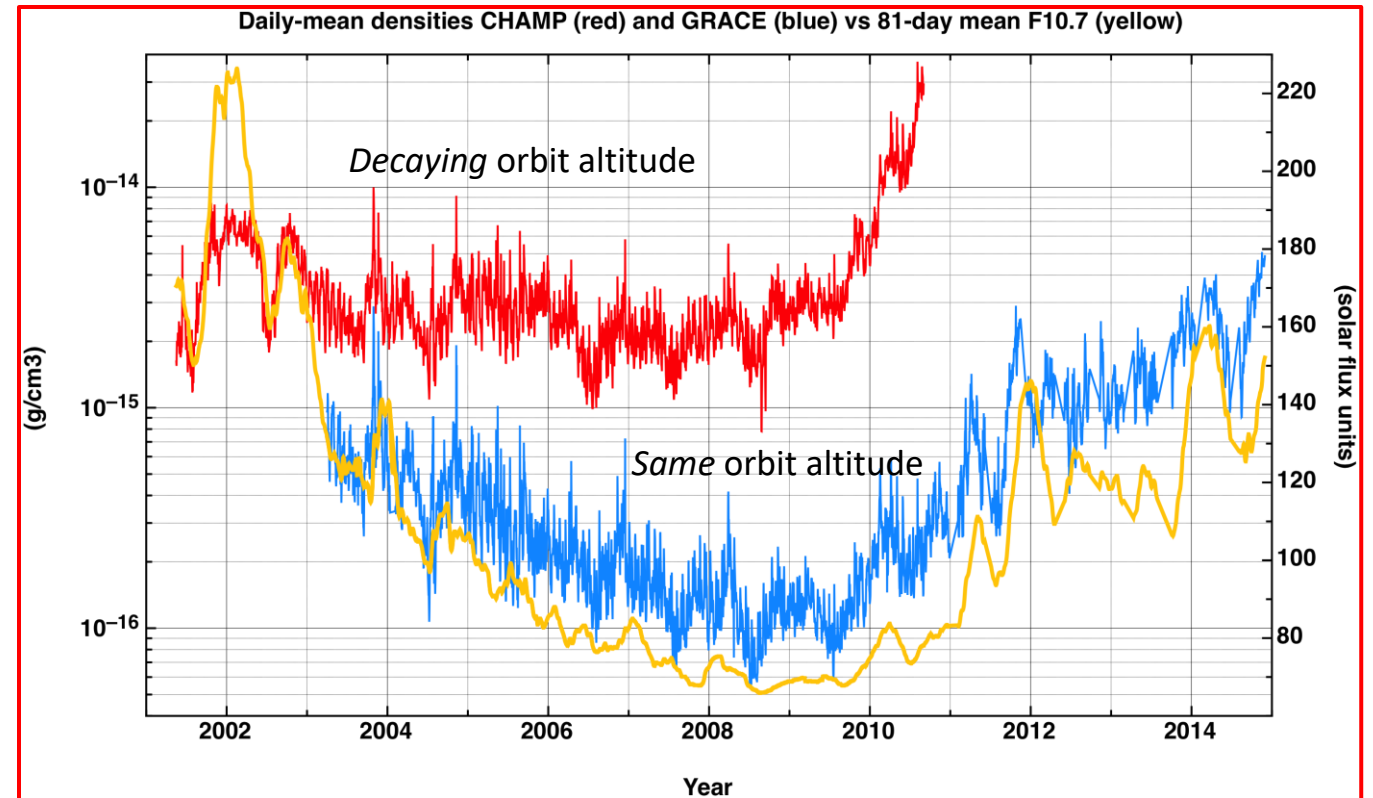




# Thermosphere density: variability

## Slow and fast temporal variations:

- Solar cycle ( $\approx 11$  years)
- Season (6 months & 12 months)
- Active regions (months)
- Solar rotation ( $\approx 27$  days)
- Corotating Interaction Regions (9 & 13.5 days)
- Day to day variations
- Solar/geomagnetic storms (hours – days)
- Solar flares (hours)

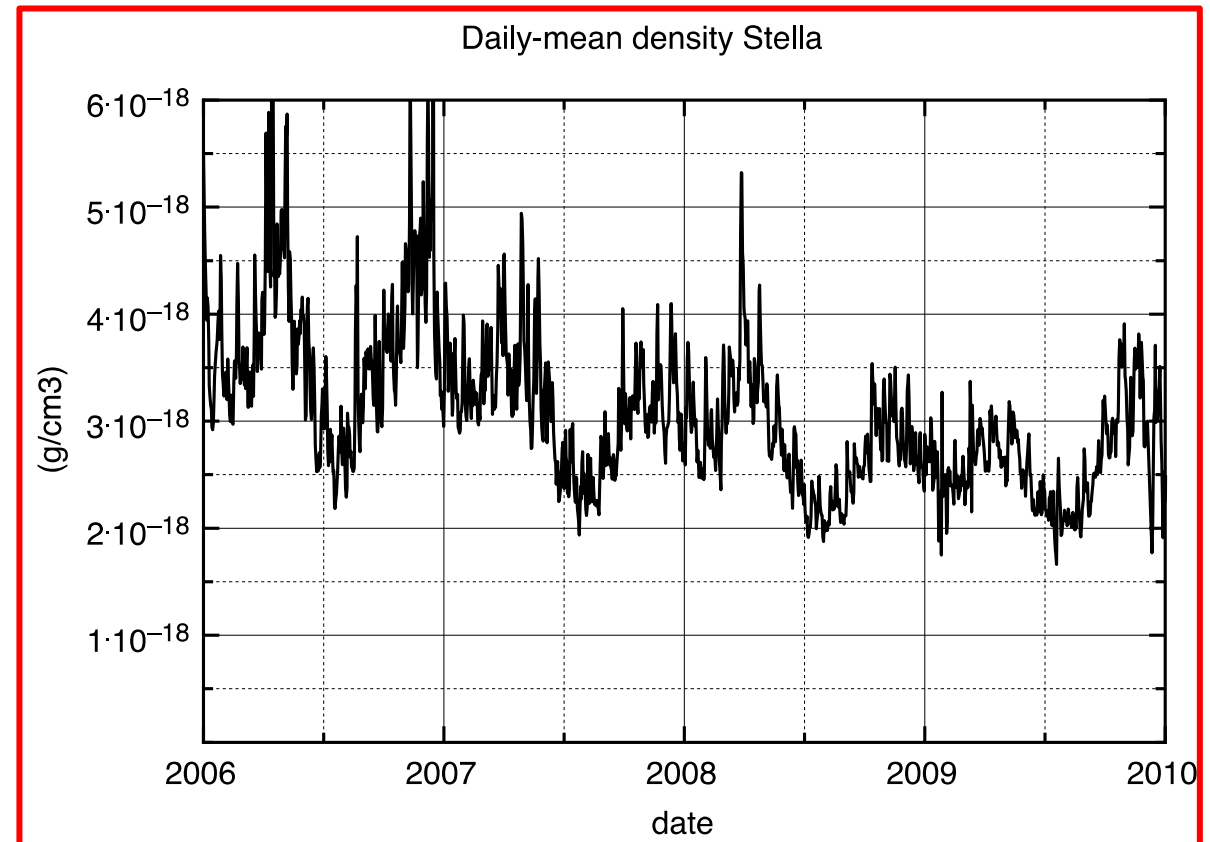




# Thermosphere density: variability

## Slow and fast temporal variations:

- Solar cycle ( $\approx 11$  years)
- Season (6 months & 12 months)
- Active regions (months)
- Solar rotation ( $\approx 27$  days)
- Corotating Interaction Regions (9 & 13.5 days)
- Day to day variations
- Solar/geomagnetic storms (hours – days)
- Solar flares (hours)

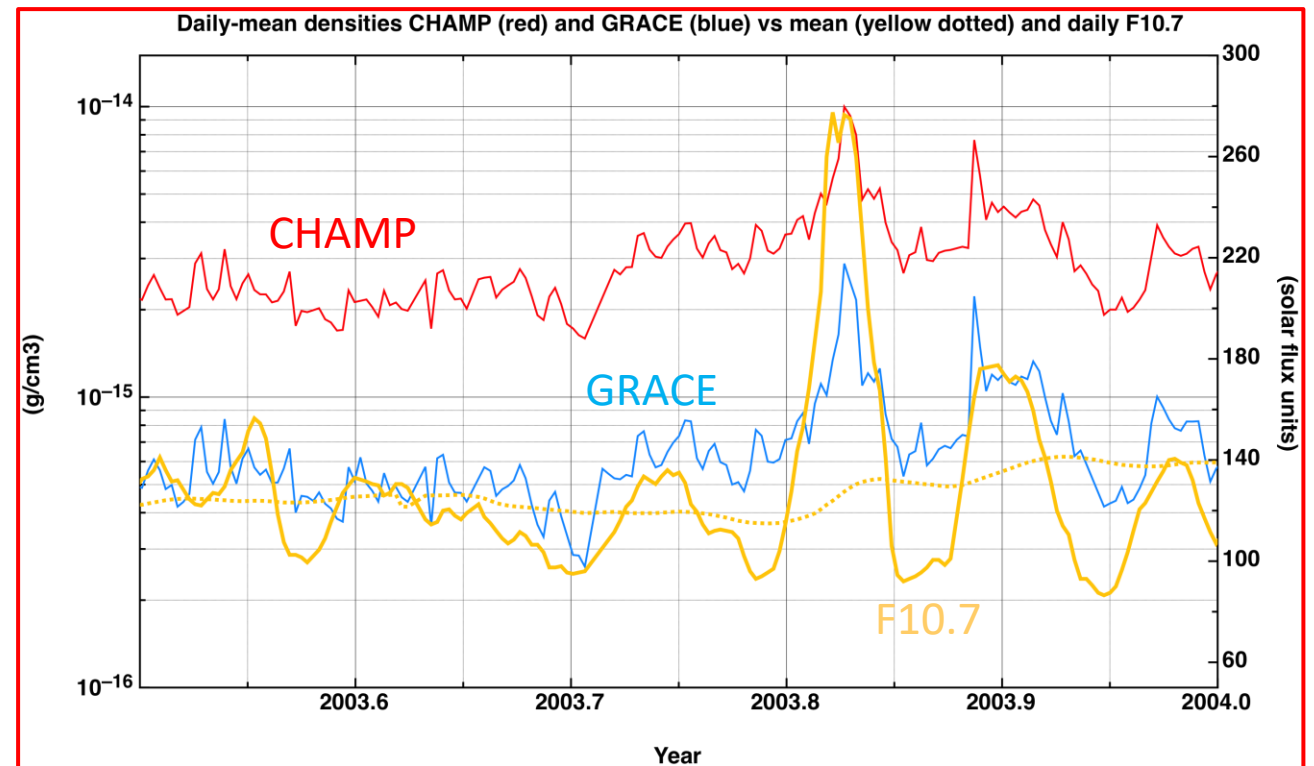




# Thermosphere density: variability

## Slow and fast temporal variations:

- Solar cycle ( $\approx 11$  years)
- Season (6 months & 12 months)
- Active regions (months)
- **Solar rotation ( $\approx 27$  days)**
- Corotating Interaction Regions (9 & 13.5 days)
- Day to day variations
- Solar/geomagnetic storms (hours – days)
- Solar flares (hours)





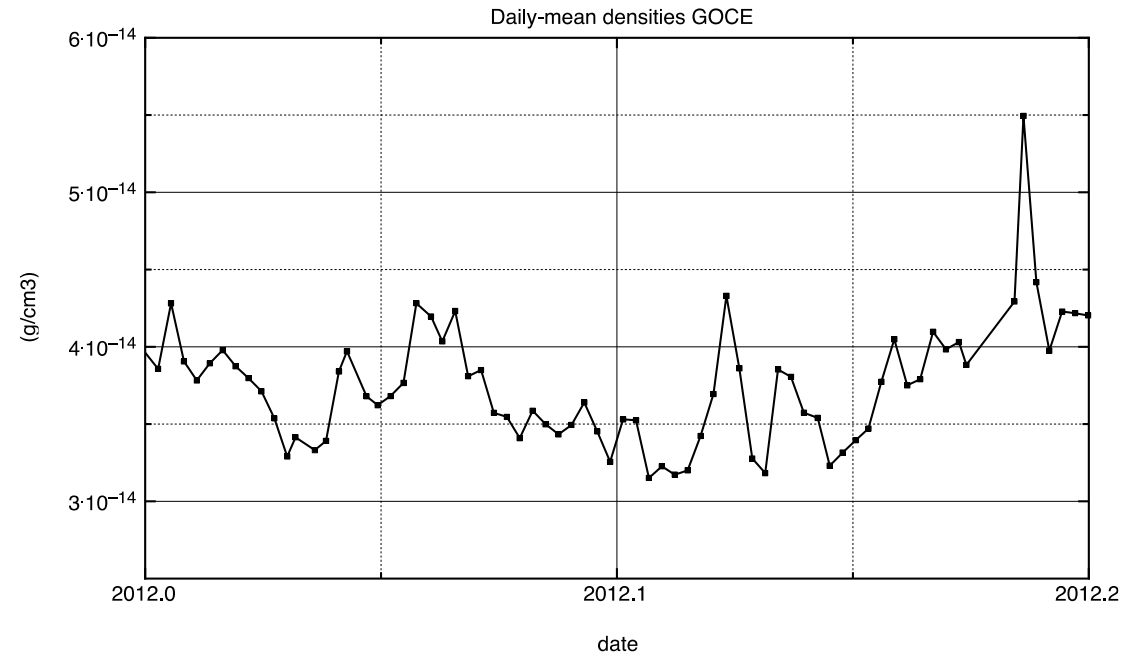
# Thermosphere density: variability

## Slow and fast temporal variations:

- Solar cycle ( $\approx 11$  years)
- Season (6 months & 12 months)
- Active regions (months)
- Solar rotation ( $\approx 27$  days)
- Corotating Interaction Regions (9 & 13.5 days)
- Day to day variations
- Solar/geomagnetic storms (hours – days)
- Solar flares (hours)

(date)	( 8 3-hourly Kp)								( 8 3-hourly ap)									
(F10.7)																		
2023 05 01	2.667	1.333	2.333	1.333	1.333	2.000	2.333	3.333	12	5	9	5	5	7	9	18	9	147.9
2023 05 02	3.000	3.000	2.000	2.667	1.000	0.667	1.333	1.000	15	15	7	12	4	3	5	4	8	156.8
2023 05 03	0.000	0.000	0.333	0.333	0.667	0.667	0.667	1.667	0	0	2	2	3	3	3	6	2	156.2

➤ Due to daily changes in geomagnetic and solar activity



➤ And due to a superposition of tidal components

Explained at the end of the presentation in A(ppendix)2



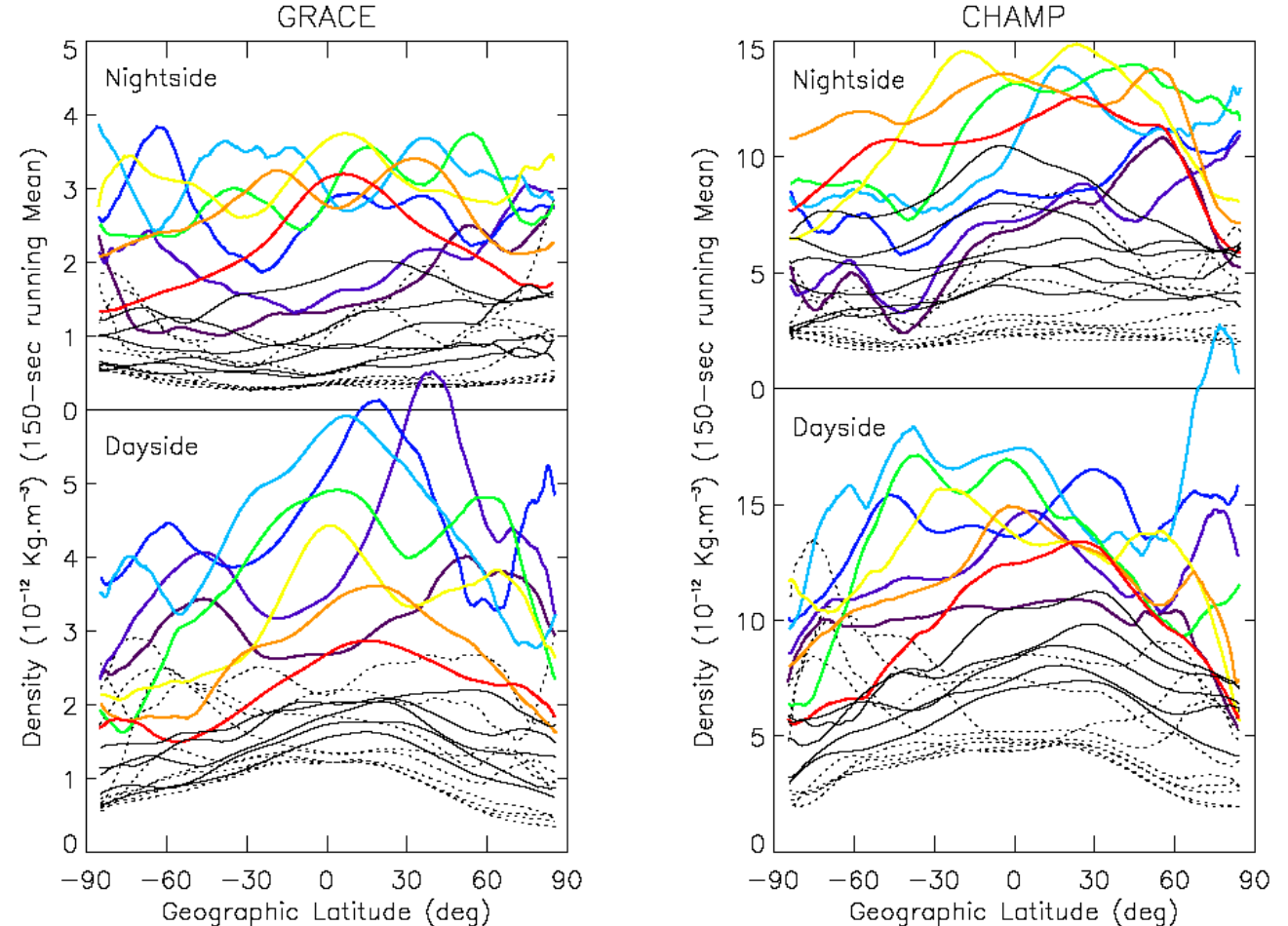
# Thermosphere density: variability

## Slow and fast temporal variations:

- Solar cycle ( $\approx 11$  years)
- Season (6 months & 12 months)
- Active regions (months)
- Solar rotation ( $\approx 27$  days)
- Corotating Interaction Regions (9 & 13.5 days)
- Day to day variations
- **Solar/geomagnetic storms (hours – days)**
- Solar flares (hours)

## Geomagnetic storm: 19-21 November 2003

Global increase in density + large-scale waves



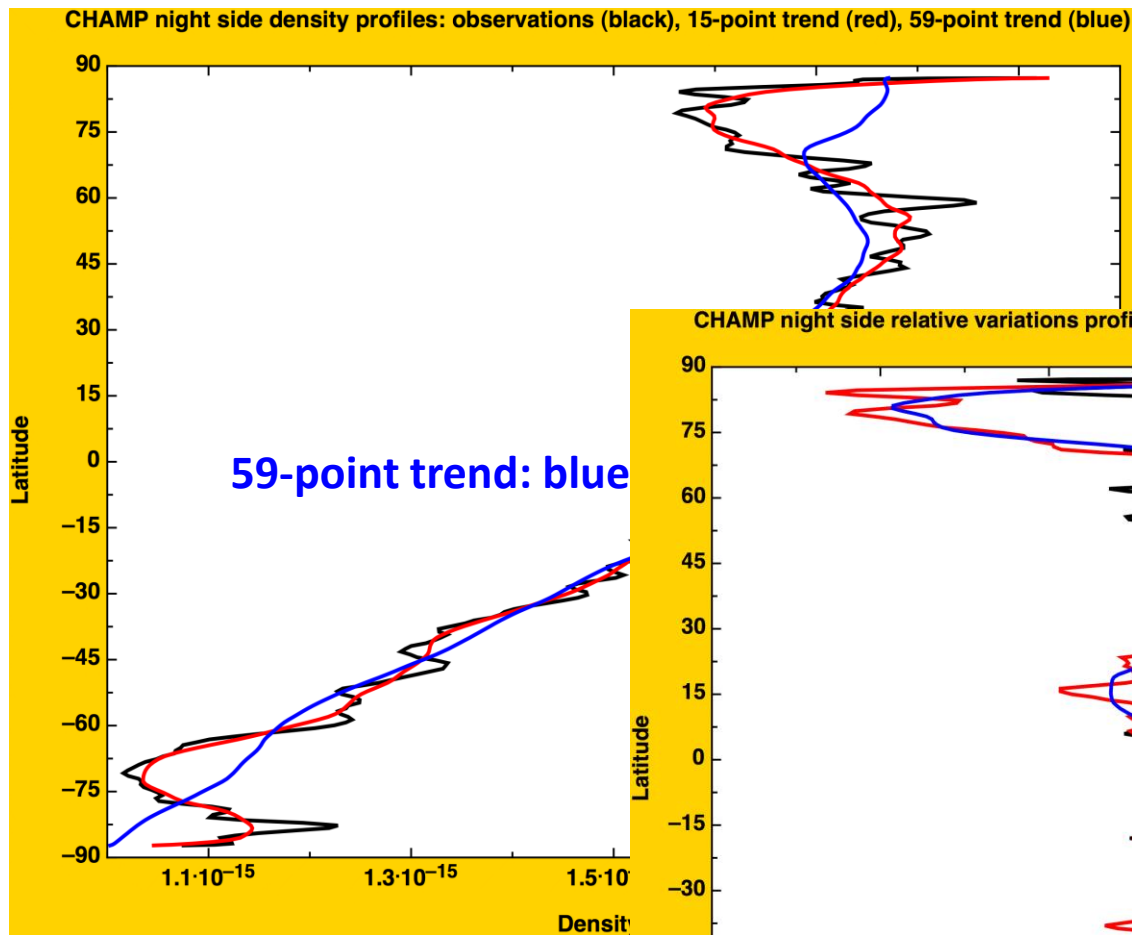
(150-sec ( $\sim 1200$  km) running means applied to raw data)



# Thermosphere density: variability

We can localize and quantify the wave-like perturbations by computing relative density variations

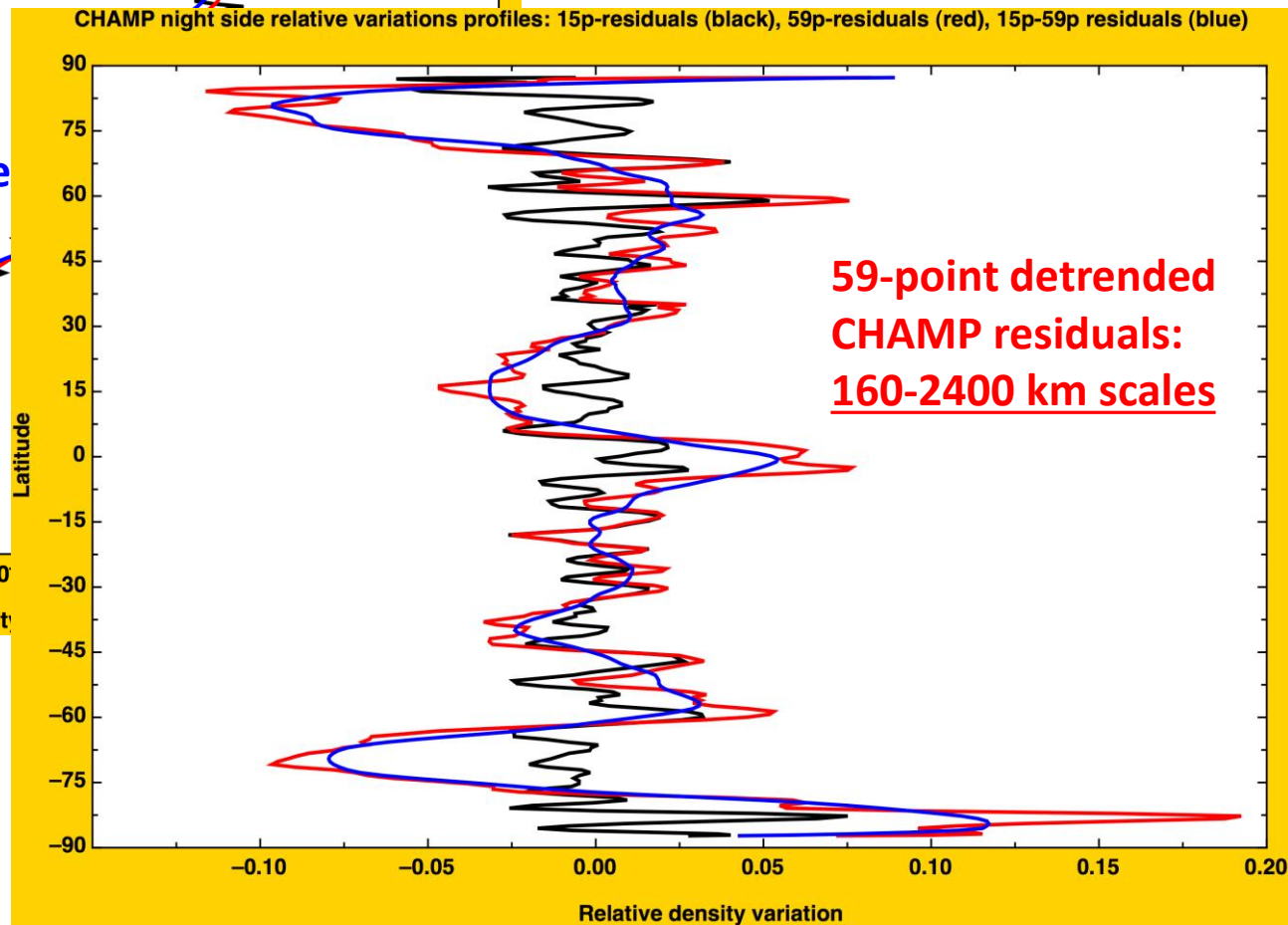
First, the trend



By detrending the data, we extract specific scales.

$$\text{Residual} = \text{observation} - \text{trend}$$

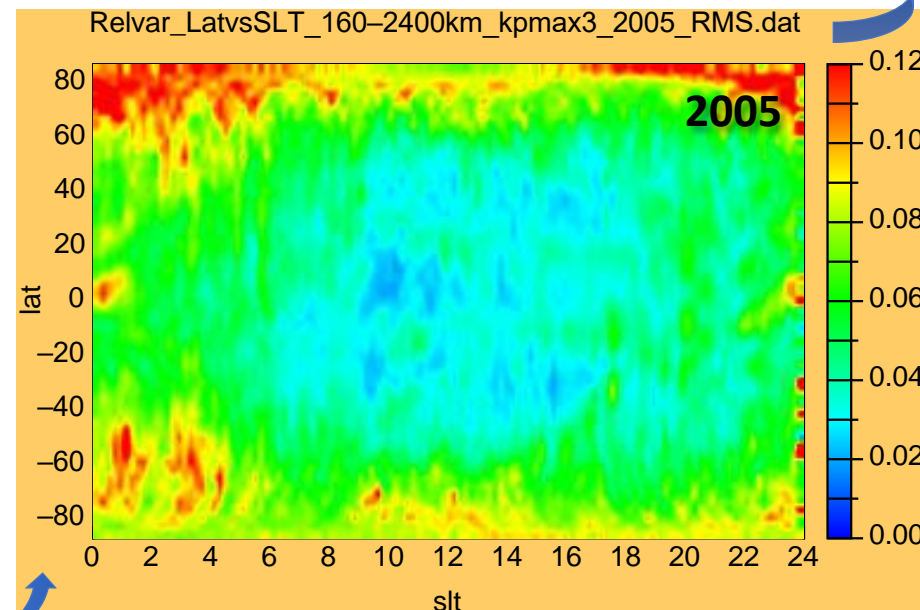
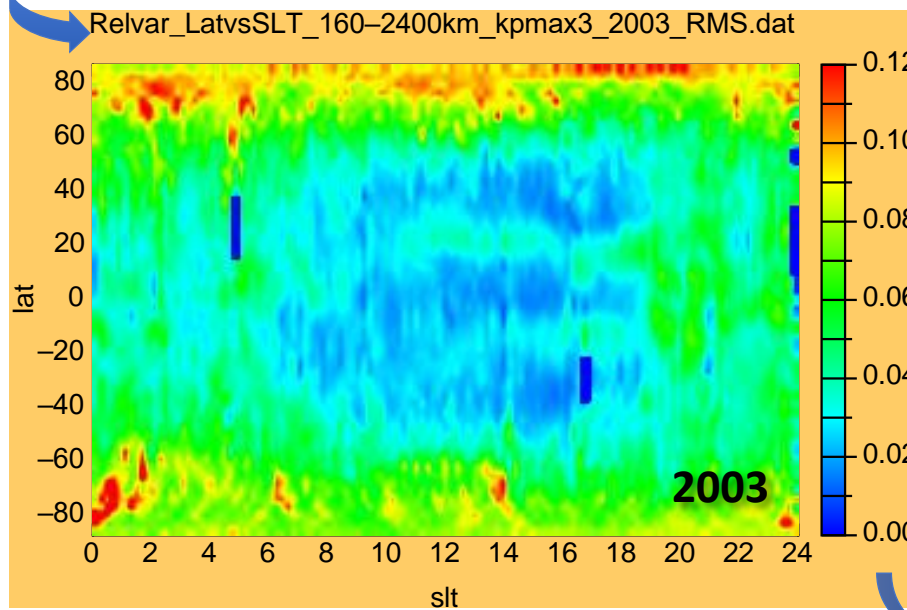
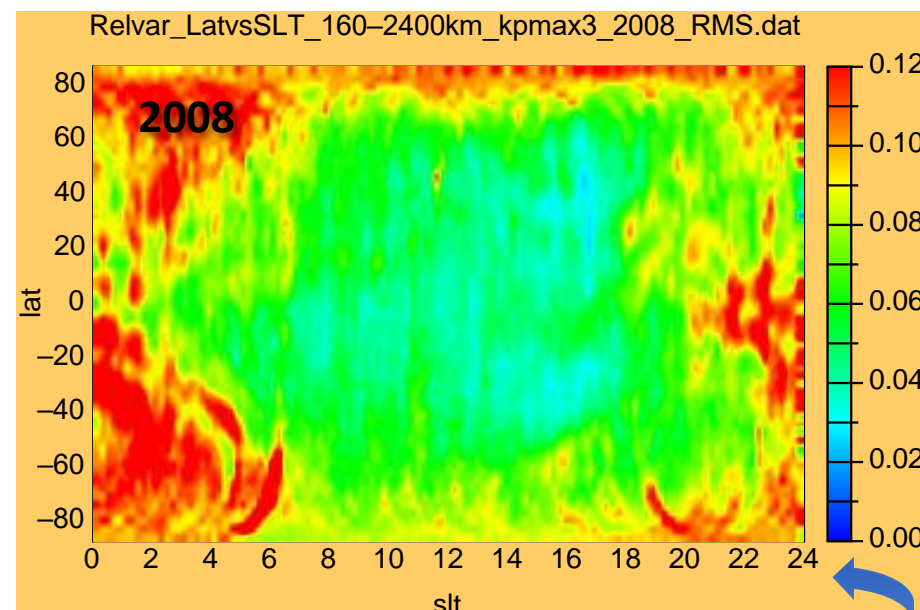
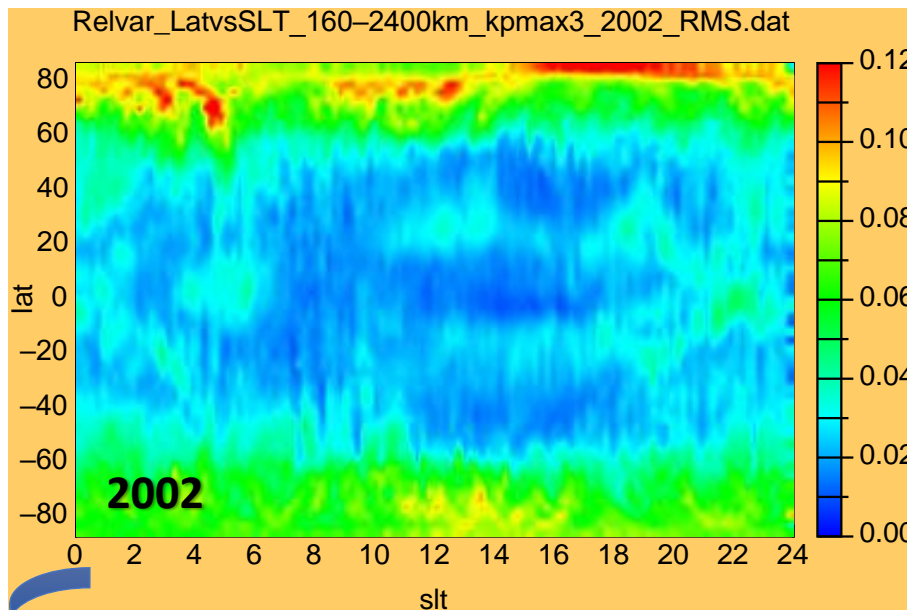
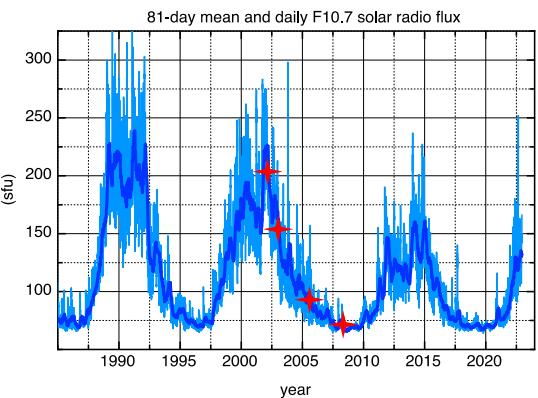
$$\text{Relative variation} = \frac{\text{residual}}{\text{trend}}$$





# Thermosphere density: variability

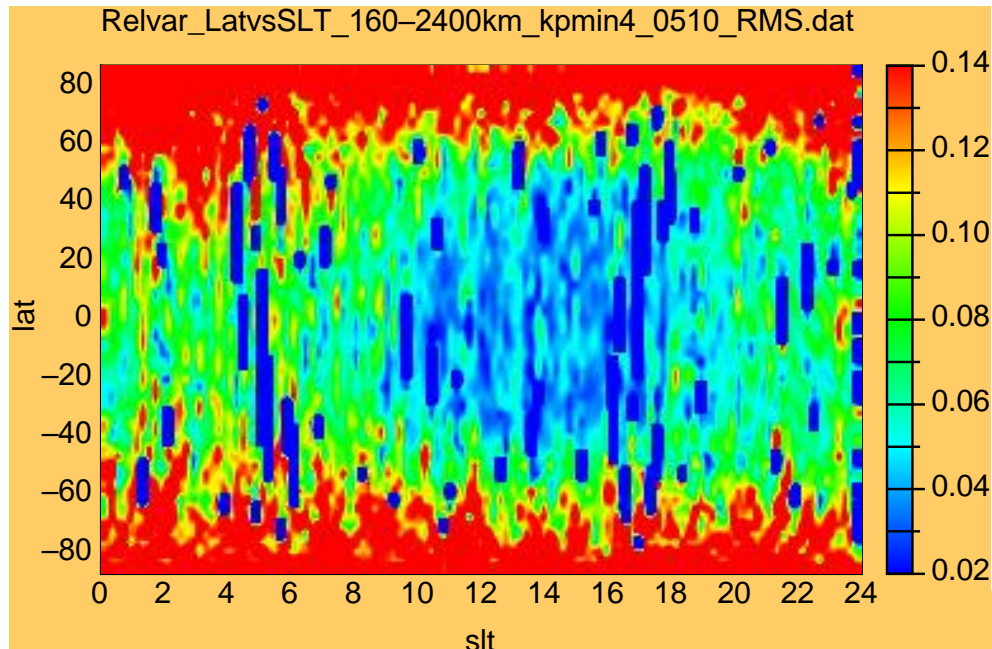
Density variability:  
CHAMP,  $K_p < 3$





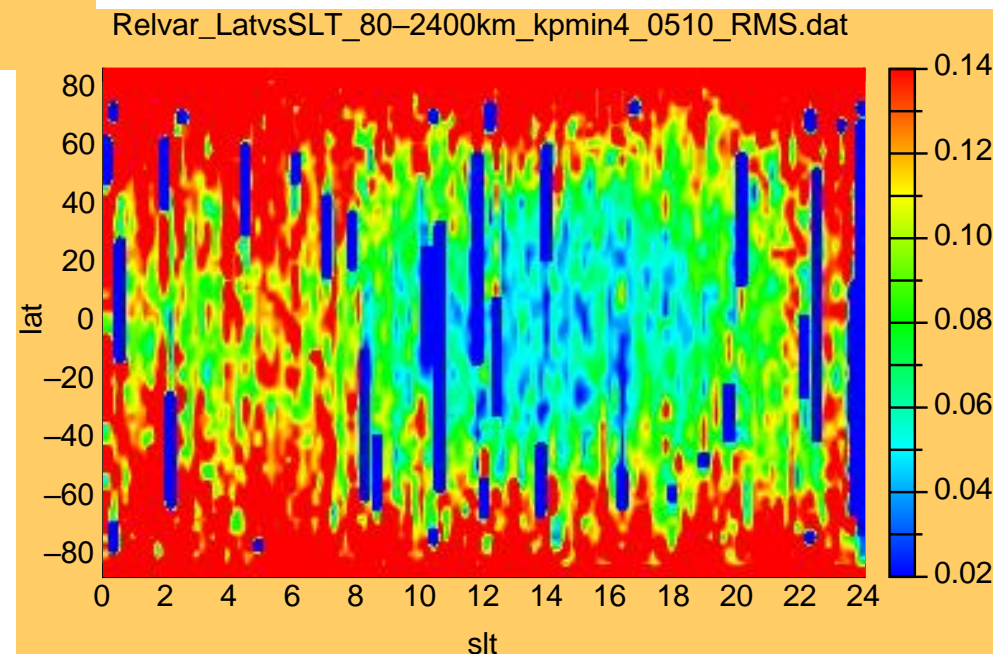
# Thermosphere density: variability

Density variability:  
CHAMP,  $K_p > 4+$



CHAMP 2005-2010

Density variability:  
GRACE,  $K_p > 4+$



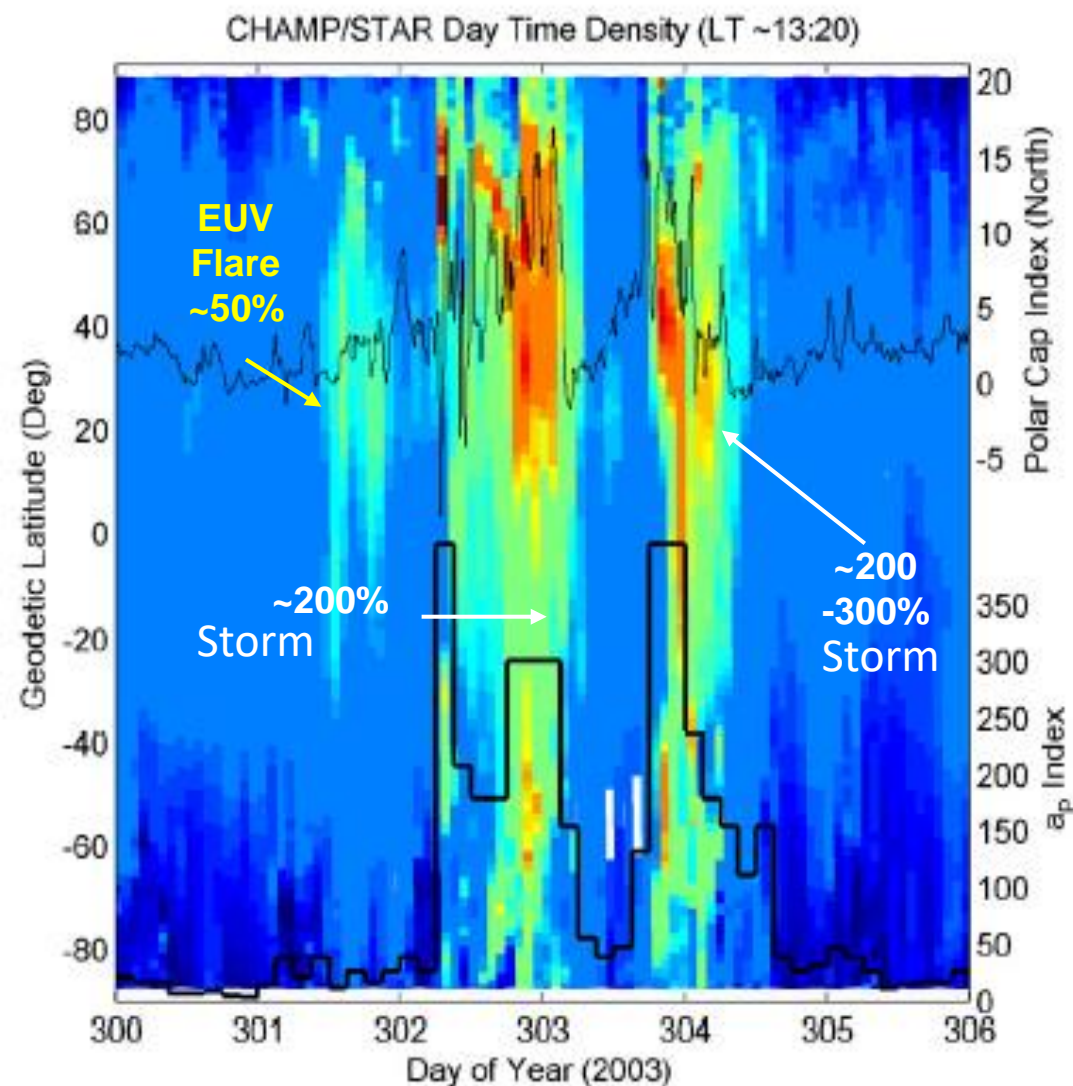
Mean altitude:  
340 km  
485 km  
GRACE 2005-2010



# Thermosphere density: variability

## Slow and fast temporal variations:

- Solar cycle ( $\approx 11$  years)
- Season (6 months & 12 months)
- Active regions (months)
- Solar rotation ( $\approx 27$  days)
- Corotating Interaction Regions (9 & 13.5 days)
- Day to day variations
- Solar/geomagnetic storms (hours – days)
- **Solar flares (hours)**



\* Thermosphere Density Response to the October 29-31 2003 Storms from CHAMP Accelerometer Measurements (*Sutton et al., JGR, 2005*)



# Summary of basic thermosphere characteristics

- Solar heating is the main energy source
- Main cooling is through molecular conduction; secondary, radiative cooling by O, CO<sub>2</sub>, NO
- Main gases: O, O<sub>2</sub>, N<sub>2</sub>, He (high altitudes only)
- Strong variability of temperature, winds and composition with solar cycle, season, local time, geomagnetic activity
- The seasonal composition changes are controlled primarily by global winds, the diurnal ones by photochemistry
- At low latitudes effects of upward propagating tides, planetary waves and gravity waves are most important (but still rather small)
- At high latitudes, heating from the magnetosphere occurs in the form of Joule heating and precipitating particles (*NB: can be equal to solar heating for severe storms*)



# Thank you for your attention

## Questions?



The PITHIA-NRF project has received funding from the European Union's Horizon 2020 research and innovation programme under grant agreement No 101007599



# Hydrostatic equilibrium

$$P \frac{dP}{dh} = -nmg$$

$g$  = gravity:  $9.81 \text{ m s}^{-2}$  (at the surface)  
 $k$  = Boltzmann constant:  $1.38 \text{ J K}^{-1} \text{ mol}^{-1}$   
 $R$  = Molar gas constant:  $8.314 \text{ J K}^{-1}$

Assuming the ideal gas law holds:

$$P = nkT$$

Then the previous expression may be written:

$$\frac{1}{P} \frac{dP}{dh} = -\frac{1}{H}$$

*integrating* 

where  $H$  is called the scale height  
(general way to describe how a value fades away,  
it is the distance for density to drop by  $1/e = 0.37$ )

$$H = \frac{kT}{mg} = \frac{RT}{g}$$



# Hydrostatic equilibrium

Leads to the so-called hydrostatic law or barometric law:

→  $P = P_0 e^{-z}$        $z = \int_0^h \frac{dh}{H}$        $z$  is referred to as the "reduced height"; the subscript zero refers to a reference height at  $h = 0$ .

Similarly,  $n = n_0 \left( \frac{T_0}{T} \right) e^{-z}$

For an isothermal atmosphere, then,

$$P = P_0 e^{-h/H}$$

$$n = n_0 e^{-h/H}$$

$$\rho = \rho_0 e^{-h/H}$$

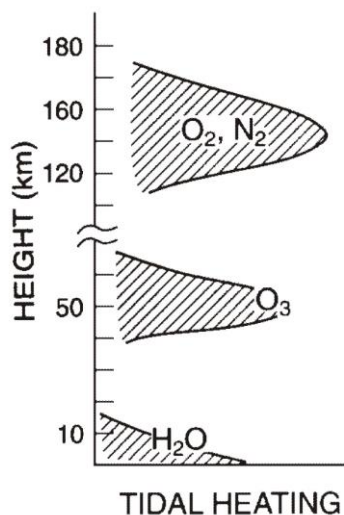
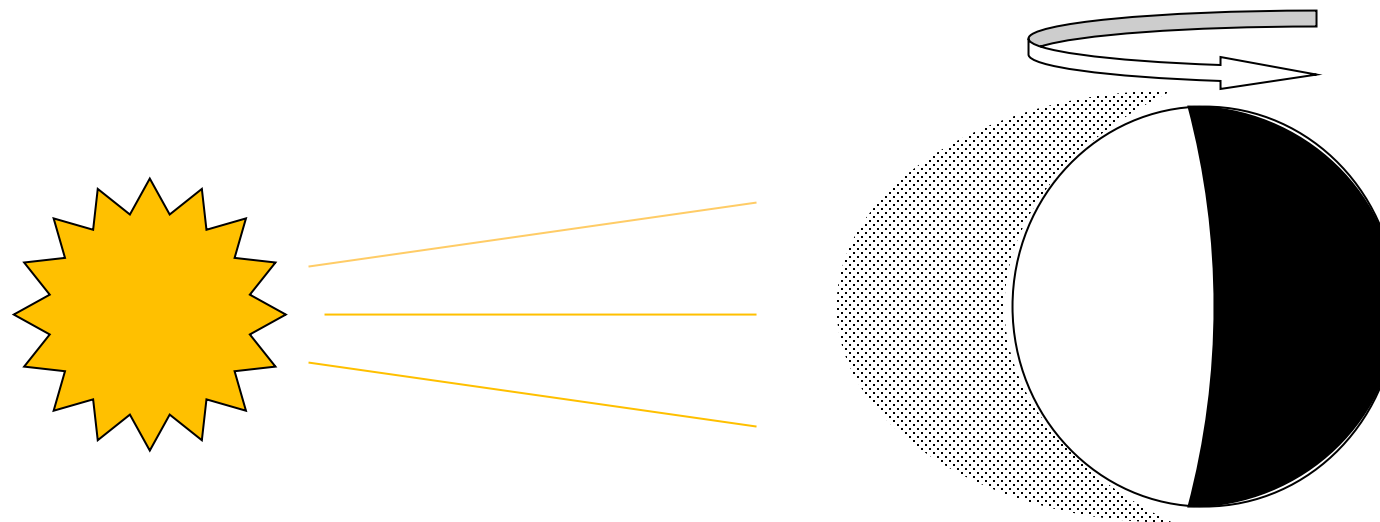


# Thermosphere density: variability

Slow and fast temporal variations:

- Solar cycle ( $\approx 11$  years)
- Season (6 months & 12 months)
- Active regions (months)
- Solar rotation ( $\approx 27$  days)
- Corotating Interaction Regions (9 & 13.5 days)
- **Day to day variations**
- Solar/geomagnetic storms (hours – days)
- Solar flares (hours)

➤ **Due to a superposition of tidal components**



Solar thermal tides are excited in a planetary atmosphere through the periodic (local time, longitude) absorption of solar radiation.

In general, tides are capable of propagating vertically to higher, less dense, regions of the atmosphere; the oscillations grow exponentially with height.

The tides are dissipated by molecular diffusion above 100 km, their exponential growth with height ceases, and they deposit mean momentum and energy into the thermosphere.



# Thermosphere density: variability

Slow and fast temporal variations:

- Solar cycle ( $\approx 11$  years)
- Season (6 months & 12 months)
- Active regions (months)
- Solar rotation ( $\approx 27$  days)
- Corotating Interaction Regions (9 & 13.5 days)
- Day to day variations
- Solar/geomagnetic storms (hours – days)
- Solar flares (hours)

➤ Due to a superposition of tidal components

To be complete:

if the excitation also depends on longitude, the spectrum of tides that is produced is more generally expressed as a linear superposition of waves of various frequencies ( $n$ ) and zonal wavenumbers ( $s$ ):

$$\sum_{s=-k}^{s=+k} \sum_{n=1}^N A_n \cos(n\Omega t + s\lambda - \phi)$$

$\lambda = \text{longitude}$

$\Omega = 2\pi/24$   
(rotating planet)

The waves with  $s = n$  are referred to as migrating tides because they migrate with respect to the Sun to a planetary-fixed observer. ( $n=1$ : diurnal /  $n=2$ : semidiurnal)

The waves with  $s \neq n$  are referred to as non-migrating tides because they do not migrate with respect to the Sun to a planetary-fixed observer

They can migrate *westward* (slower or faster than the Sun), *eastward*, or they can be *standing waves* for  $s=0$ .

NB: non-migrating tides are very small in the thermosphere above 200 km, a few percent



# References

## Empirical models

- Emmert, JT, DP Drob, JM Picone et al. (2020), NRLMSIS 2.0: A whole-atmosphere empirical model of temperature and neutral species densities, *Earth Space Sci.*, 8, 3, e2020EA001321, <https://doi.org/10.1029/2020EA001321>
- Picone, J. M., Hedin, A. E., Drob, D. P., & Aikin, A. C. (2002), NRLMSISE-00 empirical model of the atmosphere: Statistical comparisons and scientific issues. *Journal of Geophysical Research*, 107(A12), 1468. doi:doi:10.1029/2002JA009430.
- Bowman, BR, WK Tobiska, F Marcos, CY Huang, CS Lin, WJ Burke (2008) A New Empirical Thermospheric Density Model JB2008 Using New Solar and Geomagnetic Indices. Presentation at AIAA/AAS Astrodynamics Specialist Conference, Honolulu, Hawaii. <https://doi.org/10.2514/6.2008-6438>
- Bruinsma, S, and C Boniface (2021) The DTM2020 thermosphere models, *J. Space Weather Space Clim.*, 11, 47, <https://doi.org/10.1051/swsc/2021032>
- Boniface, C, S Bruinsma (2021) Uncertainty quantification of the DTM2020 thermosphere model, *J. Space Weather Space Clim.*, 11, 53, doi: 10.1051/swsc/2021034
- Storz, MF, BR Bowman, MJI Branson, SJ Casali, WK Tobiska (2005) High accuracy satellite drag model (HASDM), *Adv. Space Res.*, 36, 12, 2497-2505, <https://doi.org/10.1016/j.asr.2004.02.020>.
- Licata, RJ, PM Mehta, WK Tobiska, S Huzurbazar (2022a) Machine-Learned HASDM Model with Uncertainty Quantification, *Space Weather*, 20, 4, [doi:10.1029/2021SW002915](https://doi.org/10.1029/2021SW002915)
- Licata, RJ, PM Mehta, DR Weimer, WK Tobiska, J Yoshii (2022b) MSIS-UQ: Calibrated and enhanced NRLMSIS 2.0 model with uncertainty quantification, *Space Weather*, 20, 11, e2022SW003267. <https://doi.org/10.1029/2022SW003267>



# References

## Physical models

Qian, L., Burns, A.G., Emery, B.A., Foster, B., Lu, G., Maute, A., Richmond, A.D., Roble, R.G., Solomon, S.C., & Wang, W. (2014), The NCAR TIE-GCM: A community model of the coupled thermosphere/ionosphere system. *Modeling the Ionosphere-Thermosphere System*, J. Huba, R. Schunk, and G. Khazanov, eds., AGU Geophysical Monograph Series, 201, 73. doi:10.1002/9781118704417.ch7

Richmond, A. D., Ridley, E. C., & Roble, R. G. (1992), A thermosphere/ionosphere general circulation model with coupled electrodynamics. *Geophysical Research Letters*, 19, 601. doi: 10.1029/92GL00401

Liu, H.-L., et al. (2010), Thermosphere extension of the whole atmosphere community climate model, *J. Geophys. Res.*, 115, A12302, doi:10.1029/2010JA015586.

Akmaev, RA, TJ Fuller-Rowell, F Wu, JM Forbes, X Zhang, AF Anghel, MD Iredell, S Moorthi, HM Juang (2008) Tidal variability in the lower thermosphere: Comparison of Whole Atmosphere Model (WAM) simulations with observations from TIMED, *Geophys. Res. Lett.*, 35, L03810, doi:10.1029/2007GL032584.

Fang, TW, A Kubaryk, D Goldstein, Z Li, T Fuller-Rowell, G Millward et al. (2022) Space Weather Environment during the SpaceX Starlink Satellite Loss in February 2022, *Space Weather*, 20, 11, <https://doi.org/10.1029/2022SW003193>

Codrescu, M. V., C. Negrea, M. Fedrizzi, T. J. Fuller-Rowell, A. Dobin, N. Jakowsky, H. Khalsa, T. Matsuo, and N. Maruyama (2012), A real-time run of the Coupled Thermosphere Ionosphere Plasmasphere Electrodynamics (CTIPE) model, *Space Weather*, 10, S02001, doi:10.1029/2011SW000736.

Jin, H., et al (2011), Vertical connection from the tropospheric activities to the ionospheric longitudinal structure simulated by a new Earth's whole atmosphere-ionosphere coupled model, *J. Geophys. Res.*, 116, A01316, doi:[10.1029/2010JA015925](https://doi.org/10.1029/2010JA015925).



# References

## Indices

Tapping, KF (2013) The 10.7 cm solar radio flux (F10.7), *Space Weather*, 11, pp. 394–406, doi: 10.1002/swe.20064

Dudok de Wit, T, S Bruinsma (2017) The 30 cm radio flux as a solar proxy for thermosphere density modelling, *J. Space Weather Space Clim.*, 7, A9, doi:10.1051/swsc/2017008

Matzka, J., Stolle, C., Yamazaki, Y., Bronkalla, O., & Morschhauser, A. (2021). The geomagnetic Kp index and derived indices of geomagnetic activity. *Space Weather*, 19, e2020SW002641. <https://doi.org/10.1029/2020SW002641>

Yamazaki, Y, J Matzka, C Stolle, G Kervalishvili, J Rauberg, O Bronkalla, A Morschhauser, S Bruinsma, YY Shprits, DR Jackson (2022) Geomagnetic activity index Hpo, *Geophys. Res. Lett.*, 49, 10, <https://doi.org/10.1029/2022GL098860>

Warren, HP, JT Emmert, NA Crump (2017) Linear forecasting of the F10.7 proxy for solar activity, *Space Weather*, 15, pp. 1039–1051, doi:10.1002/2017SW001637

Henney, CJ, WA Toussaint, SM White, CN Arge (2012) Forecasting F10.7 with solar magnetic flux transport modeling, *Space Weather*, 10, 2, doi:10.1029/2011SW000748

Weimer, DR (2005) Improved ionospheric electrodynamic models and application to calculating Joule heating rates, *J. Geophys. Res.*, 110, A05306, doi:10.1029/2004JA010884

Richmond, AD (1992) Assimilative mapping of ionospheric electrodynamics, *Adv. Space. Res.*, 12, 59–68, [https://doi.org/10.1016/0273-1177\(92\)90040-5](https://doi.org/10.1016/0273-1177(92)90040-5)

Shprits, YY, R Vasile, IS Zhelayskaya (2019) Nowcasting and predicting the Kp index using historical values and real-time observations, *Space Weather*, 17, 8, 1219–1229, <https://doi.org/10.1029/2018SW002141>



# References

## Density data

Jacchia, LG, and J Slowey (1963) Accurate drag determinations for eight artificial satellites : atmospheric densities and temperatures, Smithsonian Contributions to Astrophysics, 8 (1):1–99. <https://doi.org/10.5479/si.00810231.8-1.1>

Emmert, JT, MS Dhadly, AM Segerman (2021) A globally averaged thermospheric density data set derived from two-line orbital element sets and special perturbations state vectors, J. Geophys. Res., 126, e2021JA029455, <https://doi.org/10.1029/2021JA029455>

Doornbos E (2011) Thermospheric density and wind determination from satellite dynamics, Ph.D. Dissertation, 188 pp., University of Delft, <http://repository.tudelft.nl/>.

Bruinsma, SL, E Doornbos, BR Bowman (2014) Validation of GOCE densities and thermosphere model evaluation, Adv. Space Res., 54, 576-585, <https://doi.org/10.1016/j.asr.2014.04.008>

Tobiska, WK, BR Bowman, SD Bouwer, A Cruz, K Wahl, MD Pilinski, PM Mehta, RJ Licata (2021) The SET HASDM density database, Space Weather, 19, e2020SW002682. <https://doi.org/10.1029/2020SW002682>

Van den Ijssel, J, E Doornbos, E Iorfida, G March, C Siemes, O Montenbrück (2020) Thermosphere densities derived from Swarm GPS observations, Adv. Space Res., 65, 7, 1758-1771, <https://doi.org/10.1016/j.asr.2020.01.004>

Siemes, C., et al. (2023) New thermosphere neutral density and crosswind datasets from CHAMP, GRACE and GRACE-FO, J. Space Weather Space Clim., <https://doi.org/10.1051/swsc/2023014>

Bruinsma, S, C Siemes, JT Emmert, MG Mlynczak (2022) Description and comparison of 21st century thermosphere data, Adv. Space Res., <https://doi.org/10.1016/j.asr.2022.09.038>



# References

## Solar cycle predictions

Kane, RP (2007) A preliminary estimate of the size of the coming solar cycle 24, based on ohl's precursor method, *Solar Physics*, 243, 205-217, doi:10.1007/s11207-007-0475-4

Pesnell, WD (2012) Solar Cycle Predictions, *Solar Physics*, 281, 507–532, doi: 10.1007/s11207-012-9997-5

Pesnell, WD (2016) Predictions of solar cycle 24: How are we doing?, *Space Weather*, 14, 1, 10-21, doi:10.1002/2015SW001304

Petrovay, K (2020) Solar cycle prediction, *Living Reviews in Solar Physics*, 17:2, doi: 10.1007/s41116-020-0022-z

## Reviews

Bruinsma, S., Dudok de Wit, T., Fuller-Rowell, T., Garcia-Sage, K., Mehta, P., Schiemenz, F., Shprits, Y.Y., Vasile, R., Yue, J., Elvidge, S. (2023)

Thermosphere and satellite drag, *Adv. Space Res.*, <https://doi.org/10.1016/j.asr.2023.05.011>

Emmert, J.T. (2015) Thermospheric mass density: a review, *Adv. Space Res.*, <https://doi.org/10.1016/j.asr.2015.05.038>